Article

Cell Disruption and Hydrolysis of *Microchloropsis salina* Biomass as a Feedstock for Fermentation

Ayşe Koruyucu [1,2,3], Tillmann Peest [1], Emil Korzin [1,3], Lukas Gröninger [1], Patricia [1], Thomas Brück [2,3,4] and Dirk Weuster-Botz [1,2,3,*]

1. Chair of Biochemical Engineering, School of Engineering and Design, Technical University of Munich, 85748 Garching, Germany; ayse.koruyucu@tum.de (A.K.); tillmann.peest@tum-create.edu.sg (T.P.); emil.korzin@tum.de (E.K.); lukas.groeninger@tum.de (L.G.); patricia@tum.de (P.)
2. TUM-AlgaeTec Center, Technical University of Munich, 82024 Taufkirchen, Germany; brueck@tum.de
3. TUM Pilot Plant for Industrial Biotechnology, Technical University of Munich, 85748 Garching, Germany
4. Werner Siemens—Chair of Synthetic Biotechnology, School of Natural Sciences, Technical University of Munich, 85748 Garching, Germany
* Correspondence: dirk.weuster-botz@tum.de

Abstract: Microalgae are a promising biomass source because of their capability to fixate CO_2 very efficiently. In this study, the potential of *Microchloropsis salina* biomass as a feedstock for fermentation was explored, focusing on biomass hydrolysis by employing various mechanical and chemical cell disruption strategies in combination with enzymatic hydrolysis. Among the mechanical cell disruption methods investigated on a lab scale, namely ultrasonication, bead milling, and high-pressure homogenization, the most effective was bead milling using stainless-steel beads with a diameter of 2 mm. In this way, 87–97% of the cells were disrupted in 40 min using a mixer mill. High-pressure homogenization was also effective, achieving 86% disruption efficiency after four passes on a 30–200 L scale using biomass with 15% (w/w) solids content. Enzymatic hydrolysis of the disrupted cells using a mixture of cellulases and mannanases yielded up to 25% saccharification efficiency after 72 h. Acidic hydrolysis of undisrupted cells followed by enzymatic treatment yielded around 30% saccharification efficiency but was coupled with significant dilution of the resulting hydrolysate. Microalgal biomass hydrolysate produced was determined to have ~8.1 g L^{-1} sugars and 2.5% (w/w) total carbon, as well as sufficient nitrogen and phosphorus content as a fermentation medium.

Keywords: microalgae; mechanical cell disruption; enzymatic hydrolysis; saccharification; phosphorus elimination; elemental composition

1. Introduction

The current climate crisis and the limited supply of fossil oils demand a rapid transition to renewable and sustainable resources as raw materials in the industry. Due to the urgency of the crises and the need for international cooperation to find solutions, policymakers have already taken steps towards regulating the industry's future course. As a result, research focusing on alternative green production ways and new methods promoting a more circular economy has intensified substantially.

Biomass is a promising renewable, sustainable raw material that can aid in value creation when agricultural residues or bio-waste from biotechnological production processes are converted into valuable products. Residual biomass from various industries can be hydrolyzed to its essential components, such as monosaccharides and peptides, through chemical or mechanical decomposition. The hydrolysate can then be utilized as a feedstock for fermentation of different microorganisms to produce a variety of bio-products such as organic acids, ethanol, and microbial oils [1–6]. Photosynthetically produced biomass is particularly interesting since it reduces carbon footprint when used as a feedstock and aids in the development of carbon-neutral production processes.

Microalgae are a promising biomass source as a feedstock because of their capability to fixate CO_2 very efficiently [7] and grow with wastewater streams [8,9]. Moreover, they can grow much faster than higher plants, require no arable land, and demand less freshwater use. Utilization of microalgae hydrolysate as a fermentation medium has already been demonstrated to be feasible [10,11]. Although some microalgae are oleaginous microorganisms that can produce lipids, they have relatively low lipid productivity, resulting in the low cost-competitiveness of microalgal lipid production. It has been previously shown that microalgae cultivated photoautotrophically without nutrient limitation (nitrogen, phosphorous) can achieve significantly higher biomass productivity compared to lipid production under growth-limiting conditions [12]. Therefore, it could be more beneficial to cultivate the microalgae without nutrient limitation to be used as feedstock for fermentation processes after hydrolysis.

The marine microalgae *Microchloropsis salina* is known to achieve relatively high growth rates of $0.03 \, h^{-1}$, with an optimum salinity of $35 \, g \, L^{-1}$ at pH 7.5–8.0 [13]. These conditions naturally limit the presence of contaminants in an open culture, making it possible to use simple open cultivation systems to economically produce microalgae biomass photoautotrophically as a raw material for industrial use [14]. Additionally, the high salinity requirement of the microalgae culture enables the use of seawater as the cultivation medium, reducing freshwater consumption. *M. salina* is a single-cell species not prone to aggregate or biofilm formation [15], presenting another advantage for easy cultivation. Furthermore, it has been demonstrated recently that this strain can achieve high areal biomass productivity of $27 \, g \, m^{-2} \, d^{-1}$ (dry mass) and up to 100% CO_2 fixation efficiency when cultivated in open thin-layer cascade photobioreactors [7]. Given these benefits associated with biomass production, *M. salina* was chosen as the source of biomass for the production of microalgal biomass hydrolysate in this study.

Marine microalgae have rather complex and structurally stable cell walls, which are hard to disrupt [6,16,17]. Therefore, various mechanical and chemical cell disruption methods are examined in this study. An efficient cell disruption increases the availability of the substrates for the subsequent enzymatic hydrolysis and is, therefore, crucial for the efficient hydrolysis of the whole-cell microalgae biomass. For the mechanical disruption of highly dense *M. salina* biomass, ultrasonication, bead milling, and high-pressure homogenization were investigated. These methods were selected specifically for their effectiveness with microalgae [18] and applicability in continuous processes on an industrial scale [19]. Nonetheless, mechanical cell disruption methods are energy intensive, increasing production costs. In order to determine if a lower-cost alternative is possible without compromising on the disintegration efficiency, acidic hydrolysis of the undisrupted cells followed by enzymatic hydrolysis was also performed.

Enzymatic hydrolysis of the disrupted microalgae cells aimed for maximum saccharification efficiency of the carbohydrates in the microalgal biomass. The enzymes were selected based on the cell wall composition of *Microchloropsis* species targeting the main constituents of the cell wall, namely glucose and mannose [12,17]. For process scalability, combinations of various commercially available enzyme mixtures were tested for biomass hydrolysis.

M. salina biomass grown under nutrient-replete conditions has around 26% (w/w) carbohydrates and 50% (w/w) proteins [12], both of which could be converted into valuable carbon sources that can be utilized in a fermentation process. This corresponds to a theoretical maximum of $65 \, g \, L^{-1}$ sugar concentration in a microalgal biomass hydrolysate produced using concentrated biomass with 250 g dry cell weight per liter. Although sugar concentrations around $20–50 \, g \, L^{-1}$ are considered typical for the waste streams or biomass hydrolysates generally used as a substrate for fermentation [20–23], such a low concentration of the carbon source is still significantly diluted in comparison to synthetic media used in industrial processes. Therefore, it is essential to keep the initial biomass density as high as possible to maximize the sugar concentration in the resulting biomass hydrolysate. Consequently, this study used high-density whole-cell microalgae paste with a $100–250 \, g \, L^{-1}$ solids content as the starting material.

A major advantage of using biomass hydrolysate as a cultivation medium is its high content of nitrogen and phosphorus in addition to carbon. These essential nutrients are required for unlimited microbial growth and are introduced into the synthetic growth media typically in the form of ammonia and phosphate salts, similarly to the use of a fertilizer in agriculture. Therefore, this study conducted an elemental analysis of the microalgal biomass hydrolysate to assess its suitability as a growth medium without the addition of these salts. Nevertheless, some fermentation processes, such as microbial oil production by oleaginous microorganisms or hydrogen production by photosynthetic microbes, require a nutrient deficiency in the cultivation medium to induce the metabolism to produce the desired product. To investigate the feasibility of using microalgae hydrolysate in such fermentation processes, phosphorus depletion of the biomass hydrolysate was also explored. Since using a precipitating agent is an easy and effective method commonly used in wastewater treatment facilities on large scales [24], phosphorus elimination using $FeCl_3$ as a precipitating agent was the preferred method in this work.

This study focuses on *M. salina* biomass hydrolysis by employing various mechanical and chemical cell disruption strategies in combination with enzymatic hydrolysis and aims to explore the potential of the resulting hydrolysate as a feedstock for fermentation. The analysis focuses mainly on the monosaccharide composition and the total protein and peptide content since these are the carbon sources that microorganisms can utilize in a subsequent fermentation.

2. Materials and Methods

2.1. Microalgae Strain and Biomass Production

The microalgae strain *Microchloropsis salina* (SAG 40.85), formerly referred to as *Nannochloropsis salina*, was acquired from the Culture Collection of Algae at the University of Göttingen (Göttingen, Germany). A modified artificial seawater (ASW) medium was used for all cultivations, including seed culture production [13]. ASW medium contained, per one liter of water, 27 g NaCl; 6.6 g $MgSO_4 \cdot 7\ H_2O$; 1.5 g $CaCl_2 \cdot 2\ H_2O$; 0.3 g urea; 0.07 g KH_2PO_4; 0.021 g $Na_2EDTA \cdot 2\ H_2O$; 0.014 g $FeCl_3 \cdot 6\ H_2O$; and 1 mL of a trace element solution with $ZnCl_2$ (0.04 g L^{-1}), H_3BO_3 (0.6 g L^{-1}), $CuCl_2 \cdot 2\ H_2O$ (0.04 g L^{-1}), $MnCl_2$ (0.4 g L^{-1}), and $(NH_4)_6Mo_7O_{24} \cdot 4\ H_2O$ (0.37 g L^{-1}).

To produce the microalgal biomass used in this study, *M. salina* was cultivated in open thin-layer cascade photobioreactors using ASW medium under nutrient-replete conditions and physical simulation of outdoor climate conditions of a summer day in June 2012 in Almería, Spain. The biomass was then dewatered using a dynamic settler with spiral plate technology (Evodos 50A, Evodos B.V., Raamsdonksveer, The Netherlands), allowing the harvest of a microalgae paste with ~30% cell dry weight. The biomass was stored at −20 °C until further use. The exact cultivation and harvesting conditions were described previously in detail [7].

2.2. Mechanical Cell Disruption

2.2.1. Ultrasonication

A sonotrode (Sonopuls, Bandelin electronic GmbH, Berlin, Germany) consisting of a high-frequency generator (Sonopuls GM-2070) and an ultrasonic transducer (Sonopuls UW-2070) equipped with a titanium micro tip (Sonopuls MS 73) was used for the ultrasonic disruption of microalgae cells. The parameter settings given in Table 1 were adjusted on the homogenizer device. A total of 25 mL from each sample was placed into a 50 mL centrifuge tube, placed into an ice bath to provide cooling during the treatment, and homogenized for a duration specified individually for each experiment in the results.

Table 1. Parameter settings for disruption of *M. salina* cells with an ultrasonic homogenizer.

Sonotrode	Power	Frequency	Amplitude	Pulsation
MS73	70 W	20 kHz	97%	100%

2.2.2. Bead Beating

For the disruption of microalgal cells through bead milling, a mixer mill (MM 400, Retsch GmbH, Haan, Germany) equipped with stainless-steel grinding jars with a nominal volume of 25 mL was used. Both the sample and the bead filling were at 40%, so the total filling volume of the jars was 80%, which corresponded to 20 mL. The jars were placed into an ice bath for cooling during sampling. Each sample was homogenized for a specified duration of time at a mixing frequency of 30 s^{-1}. The specifications of the various beads (Retsch GmbH, Haan, Germany) used for cell disruption are given in Table 2.

Table 2. Specifications of the various beads used for cell disruption of *M. salina* by bead milling.

Nr.	Material	Diameter, mm	Density, g mL^{-1}
1	Zirconium oxide	1	6.1
2	Zirconium oxide	0.5	6.9
3	Agate	1	6.0
4	Glass	3	2.9
5	Stainless steel	5	7.7
6	Stainless steel	2	7.7
7	Tungsten carbide	3	14.9

2.2.3. High-Pressure Homogenization

For microalgal cell disruption by high-pressure homogenization on a 200 mL scale, a tabletop high-pressure homogenizer (HPH) (HPL6, Maximator GmbH, Nordhausen, Germany) was used. In this case, 200 mL of each sample was processed at a flow rate of 4 L h^{-1} for up to 10 passes at a specified outlet pressure. For homogenization at scales larger than 30 L, an industrial HPH (Ariete NS3015H, GEA Group AG, Düsseldorf, Germany) with an external manually operated diaphragm pump (SartoJet, Sartorius AG, Göttingen, Germany) as the inlet pump was used. In this case, for practical reasons, the biomass was circulated in a tank with a cooling jacket and an external stirrer unit during homogenization. Thus, instead of counting the actual number of passes (N), the time equivalent of passes (N_E) was calculated, which was defined as the homogenization time (t_H) divided by the total volume (V) and multiplied by the volumetric flow rate (F) as follows:

$$N_E = (t_H \cdot F) \cdot V^{-1}, \tag{1}$$

The biomass was processed at a flow rate of $150–200 \text{ L h}^{-1}$ for up to 5 equivalent passes (N_E) at an outlet pressure of 1000 bar. During the homogenization process, the inlet pressure was manually adjusted to 3.5 bar at all times using a diaphragm pump.

2.3. Chemical Hydrolysis of Undisrupted Cells

Chemical hydrolysis of undisrupted *M. salina* cells was investigated using a combination of acidic and enzymatic hydrolysis. A pretreatment with proteases was performed before the hydrolysis with polysaccharide-degrading enzymes to determine if this would increase the accessibility of carbohydrates for the latter enzymes. The two different protease mixtures tested for this purpose were Protamex® (Novozymes, Bagsværd, Denmark) with maximum activity at pH 7.0 and Protease from *Aspergillus saitoi* (Sigma-Aldrich, Taufkirchen, Germany) with maximum activity at pH 3.5. Thus, the use of the latter protease was also considered as acidic hydrolysis.

Chemical hydrolysis was performed using *M. salina* biomass with a CDW concentration of 163 g L^{-1} and the commercial enzyme mixes listed in Table 3. The enzyme dosing is expressed in g enzyme per g CDW of the biomass suspension and was adjusted to 1.0% protease, 5.9% cellulase mixture, and 0.12% mannanase. Since the optimal pH and temperature conditions to achieve maximum activity differed for each enzyme, these parameters were adjusted differently for the proteolysis and the following polysaccharide hydrolysis, as listed in Table 4. The exact procedure applied was as follows:

- Adjustment of the pH to the optimum value depending on the protease used as specified in Table 4 by addition of concentrated acetic acid solution.
- Proteolysis using the specified protease mix for 18 h.
- Autoclaving at 121 °C for 20 min (for sterilization and protease inactivation).
- Adjustment to pH 5.0 by addition of concentrated potassium hydroxide solution.
- Addition of cellulase and mannanase mixtures and further hydrolysis for 72 h.

Table 3. Commercial enzymes used for enzymatic hydrolysis of microalgal biomass in combination with acidic hydrolysis.

Enzyme	Activity	Manufacturer
Cellic® CTec3 HS	Cellulase, β-glucosidase, hemicellulase	Novozymes (Bagsværd, Denmark)
Rohalase® GMP	Endo-mannanase	AB Enzymes (Darmstadt, Germany)
Protamex®	Endo-protease	Novozymes (Bagsværd, Denmark)
Protease from *Aspergillus saitoi*	Protease, β-glucosidase	Sigma-Aldrich (Taufkirchen, Germany)

Table 4. Hydrolysis conditions used for different enzymes for optimal enzyme activity according to the manufacturer's specifications.

Enzyme	pH	Temperature
Protamex®	7.0	37 °C
Protease from *Aspergillus saitoi*	3.5	37 °C
Other enzymes	5.0	50 °C

2.4. Enzymatic Hydrolysis of Mechanically Disrupted Cells

Enzymatic hydrolysis of microalgal biomass was carried out on different scales. The preliminary experimentation with various enzyme doses was performed in 5 mL screw-cap glass vials in triplicate using a thermal shaker (Thermomixer Basic, CellMedia GmbH & Co. KG, Zeitz, Germany) incubating the reaction mixture for 72 h with an agitation rate of 550 rpm. Scale-up experiments on a 60 L scale were performed in a stirred-tank reactor (LP 75 L, Bioengineering AG, Wald, Switzerland) with an agitation rate of 550 rpm. Scale-up to 200 L was done in a tempered stirred tank (M500 L, Bioengineering AG, Wald, Switzerland). The commercial enzymes used for biomass hydrolysis are listed in Table 5.

Table 5. Commercial enzymes used for enzymatic hydrolysis after mechanical cell disruption.

Enzyme	Activity	Manufacturer
Cellic® CTec3 HS	Cellulase, β-glucosidase, hemicellulase	Novozymes (Bagsværd, Denmark)
Hemicellulase from *Aspergillus niger*	Hemicellulase	Sigma-Aldrich (Taufkirchen, Germany)
Rohament® CEP	Cellulase, β-glucosidase, hemicellulase	AB Enzymes (Darmstadt, Germany)
Rohalase® GMP	Endo-mannanase	AB Enzymes (Darmstadt, Germany)
Protamex®	Endo-protease	Novozymes (Bagsværd, Denmark)

Cell dry weight (CDW) concentration of the microalgal biomass to be hydrolyzed was adjusted to 150 g L^{-1} in all cases. The cells were always mechanically disrupted by high-pressure homogenization using an industrial HPH before performing enzymatic hydrolysis unless stated otherwise. Instead of heat sterilization, antibiotics (each 100 mg L^{-1} of kanamycin sulfate and tetracycline hydrochloride) were added to the biomass at the beginning of hydrolysis to inhibit the growth of contaminants unless specified otherwise.

In some cases, pretreatment with proteases was performed before adding polysaccharide-degrading enzymes to determine if this would increase the accessibility of

carbohydrates for the latter enzymes. Since the optimal pH and temperature conditions to achieve maximum activity differed for each enzyme, these parameters were adjusted differently for the proteolysis and the following polysaccharide hydrolysis, as listed in Table 4.

2.5. Phosphorus Elimination

A phosphate precipitation method using a precipitating agent, namely $FeCl_3$, was adopted for phosphorus elimination. Initial experiments were carried out using a phosphate buffer containing 0.209 g L^{-1} Na_2HPO_4 and 0.035 g L^{-1} KH_2PO_4 corresponding to a Na_2HPO_4:KH_2PO_4 stoichiometric ratio of 5.75:1 and a phosphate concentration of 164.3 mg L^{-1}. A total of 50 mL from phosphate buffer was transferred into a 50 mL centrifugation tube, and a 0.24 M $FeCl_3 \cdot 6 H_2O$ solution was added to achieve the desired Fe:P stoichiometric ratio. The pH of the reaction mixture was adjusted to pH 4.5–5.5 by adding 3 M KOH solution. Then, the reaction mixture was thoroughly mixed using a vortex mixer and incubated for 20 min. Finally, the reaction tubes were centrifuged at 3260 rcf, and the phosphate concentration of the supernatant was measured.

Phosphate precipitation of microalgae hydrolysate was performed on a 200 L scale in a tempered stirred tank (M500L, Bioengineering AG, Wald, Switzerland) with pH monitoring. In this case, required amounts of $FeCl_3 \cdot 6 H_2O$ and KOH were added to microalgae hydrolysate in solid form to prevent a significant dilution of the resulting hydrolysate, and multiple successive precipitation steps were applied to minimize the amount of $FeCl_3$ used. Separation of the precipitated $FePO_4$ on the 200 L scale was done by centrifugation using a disk separator (CSA 08-06-476, GEA Westfalia Separator Group, Oelde, Germany).

2.6. Cell Dry Weight Measurement

Cell dry weight (CDW) of high cell density microalgae biomass (100–250 g L^{-1} CDW) with high viscosity was determined in triplicate gravimetrically by spreading a certain amount of sample onto pre-dried and pre-weighed aluminum dishes and drying for at least 72 h at 70 °C before weighing again. The CDW content was then calculated by dividing the difference in dry weight by the mass of the sample initially spread onto the dish.

2.7. Determination of Cell Disruption Degree

For quantitative evaluation of the mechanical disruption of *M. salina* cells, each sample was analyzed using a flow cytometer (CytoFLEX V0-B4-R2, Beckman Coulter GmbH, Krefeld, Germany). The proportion of intact cells and cell debris as a frequency in total incidence count was based on shifts in the measured forward-scattered light (FSC) and the fluorescence in the wavelength range of 640–780 nm (F640–780). The use of F640–780 for the analysis was based on an empirical approach making use of the fluorophore content of microalgae, such as allophycocyanin with an emission peak at 660 nm, which would presumably be released upon cell disruption [25]. In order to ensure an accurate measurement, each sample was diluted with distilled water so that its optical density measured at a wavelength of 750 nm was around 0.150, and the flow rate was adjusted to a value corresponding to less than 3000 incidences per second. Per sample, 100,000 incidences were recorded and used to plot a log-log graph of F640–780 values with respect to FSC. The areas occupied by distilled water, intact *M. salina* cells, cell debris, and an unknown fraction were marked on this dot plot to sort the incidences accordingly. The degree of cell disruption (DCD) was then calculated as:

$$DCD = i_{cells} \cdot (i_{cells} + i_{debris})^{-1}, \tag{2}$$

where i_{cells} and i_{debris} are the incidence counts of intact cells and cell debris, respectively.

2.8. Determination of Sugar, Phosphate, and Total Protein Concentrations

Each sample was centrifuged at 20,817 rcf for 5 min, and the supernatant was filtered (0.2 μm) before the substrate measurement. Concentrations of glucose and galactose were

determined photometrically using enzymatic assays (D-Glucose, Lactose/D-Galactose assay kits, R-Biopharm AG, Darmstadt, Germany). Similarly, concentrations of mannose, rhamnose, and xylose were also determined photometrically using enzymatic assays (D-Mannose/D-Fructose/D-Glucose, L-Rhamnose, and D-Xylose assay kits, Megazyme, Wicklow, Ireland). Phosphate concentration was measured using a colorimetric test kit (Phosphate colorimetric kit, Sigma-Aldrich, Taufkirchen, Germany). The total protein and peptide content of the hydrolysate was determined in duplicate using the Pierce™ BCA Protein Assay Kit (Thermo Fisher Scientific, Schwerte, Germany).

2.9. Elemental Composition

Carbon, hydrogen, nitrogen, and sulfur (CHNS) contents were analyzed using a CHNS elemental analyzer (Euro EA CHNS Elemental Analyzer, HEKAtech GmbH, Wegberg, Germany). In the analyzer, each sample was combusted using oxygen at 1800 °C, and the resulting gas mixture containing CO_2, H_2O, N_2, and SO_2 was fed into a gas chromatography column for separation using helium as carrier gas. The separated gases were measured by a thermal conductivity detector. The C, H, N, and S contents were then calculated as the mass of the element measured per mass of the initially weighed sample. Cell samples were freeze-dried for the analysis, and each sample was measured in triplicate.

Phosphorus content was determined using a colorimetric method. Samples were mineralized in round bottom flasks at 400 °C using concentrated sulfuric acid and nitric acid. Then, the nitrous gases were boiled away. An aliquot part of ammonium vanadate and ammonium molybdate was added to the mixture. The resulting phosphomolybdic acid was measured against standards photometrically at 650 nm (Cary 100 UV–Vis Spectrophotometer, Agilent, Waldbronn, Germany). Each sample was measured in duplicate.

2.10. Macromolecular Composition

The macromolecular composition of the biomass was determined using a combination of analytic data of the samples in this work and literature values. Lipid content was calculated based on measurements of CDW and lipid concentrations. Total protein content was calculated from nitrogen content using a correlation factor of 4.4 [26]. The ash content of *M. salina* biomass cultivated in a nutrient-replete medium under the same conditions as in this work was measured to be 10.0% in a previous study [12]. The remaining portion of the biomass is assumed to be carbohydrates.

The total lipid concentration of a sample was determined using the sulfo-phospho-vanillin (SPV) assay described by Mishra et al. [27]. To prepare the phospho-vanillin reagent, 0.3 g of vanillin was dissolved in 50 mL of 10% (*v/v*) ethanol in water mixture and mixed with 200 mL of phosphoric acid. A total of 50 µL from each sample was incubated in 1 mL sulfuric acid (98% (*v/v*)) for 10 min at 90 °C in glass vials and cooled at −4 °C for 5 min. Then, 2.5 mL phospho-vanillin reagent was added into each vial, and the mixture was incubated in a thermomixer at 37 °C and 900 rpm for 15 min (Thermomixer basic, CellMedia, Elsteraue, Germany). After incubation, the absorption at 530 nm wavelength against air was measured with a UV–vis spectrophotometer (Genesys 10S UV–VIS, Thermo Fisher Scientific Inc., Waltham, MA, USA). Blank values were measured separately and subtracted from the measured absorption values manually. Each sample was measured in triplicate. An external standard of rapeseed oil was used to create a correlation line between absorption and total lipid concentration. For this, different amounts of an oil in hexane solution with a known concentration (1 g L^{-1}) were transferred into glass vials. After the hexane was evaporated, 50 µL of demineralized water (same as the sample volume) was added, and the standard assay procedure described above was applied. The resulting correlation line covered a range of 0.0–2.0 g L^{-1} lipids. Cellular lipid content was calculated by dividing the total lipid concentration by CDW concentration.

2.11. Process Metrics

The efficiency of biomass hydrolysis was evaluated using two different parameters. Saccharification efficiency (η_{sac}) is defined as the ratio of sugars released from the carbohydrates in biomass to the theoretical maximum of releasable sugars and is calculated for microalgae biomass hydrolysis as follows:

$$\eta_{sac} = (c_{glu} + c_{man}) \cdot (c_X \cdot x_{X,carb} \cdot (x_{carb,glu} + x_{carb,man}))^{-1}, \tag{3}$$

where c_{glu} and c_{man} are the glucose and mannose concentrations released by hydrolysis, respectively, $x_{X,carb}$ is the carbohydrate fraction of the CDW of the microalgae, and $x_{carb,glu}$ and $x_{carb,man}$ are the glucose and mannose mass fractions in the carbohydrates of the microalgae, respectively. Here, only glucose and mannose were taken into account, since these make up over 80% of the total sugar content of *M. salina* and were the target of enzymatic hydrolysis. Schädler et al. [12] determined the sugar composition of *M. salina* grown in thin-layer cascade photobioreactors in a nutrient-replete ASW medium to be as presented in Table 6, which was used to calculate the saccharification efficiency. CDW concentration (c_X) was adjusted to 150 g L^{-1} in all hydrolysis experiments prior to cell disruption, while the carbohydrate fraction of the dry *M. salina* biomass ($x_{X,carb}$) was determined through analysis of its elemental and macromolecular composition. Since the enzyme mixes used for hydrolysis contained sugars as well, their contribution to the final sugar concentration of the biomass hydrolysate was measured and subtracted to determine the sugars released from the biomass by hydrolysis.

Table 6. Sugar composition of *M. salina* grown in thin-layer cascade photobioreactors in a nutrient-replete ASW medium [12].

Carbohydrate Moiety	Mass Fraction in CDW, mg g^{-1}	Mass Fraction in Total Sugars, %
Glucose	161.5	62.7
Mannose	50.1	19.5
Galactose	17.2	6.8
Rhamnose	12.8	5.0
Other sugars	15.9	6.0

Carbon solubilization efficiency (η_C) of the microalgal biomass, considering all carbon sources present in it, was calculated as follows:

$$\eta_C = (x_{C,MAH} \cdot \rho_{MAH}) \cdot (c_X \cdot x_{C,X})^{-1}, \tag{4}$$

where $x_{C,MAH}$ is the mass fraction of carbon in microalgae hydrolysate, ρ_{MAH} is the density of microalgae hydrolysate; c_X is the CDW concentration of microalgae biomass to be hydrolyzed, and $x_{C,X}$ is the mass fraction of carbon in dry *M. salina* biomass. The CDW concentration (c_X) was adjusted to 150 g L^{-1} in all hydrolysis experiments prior to cell disruption, while the mass fractions of carbon in the dry biomass and in the hydrolysate were determined by elemental analysis. Additionally, the density of the biomass hydrolysate (ρ_{MAH}) was measured to be 995.8 g L^{-1}.

3. Results and Discussion

3.1. Composition of M. salina Biomass

Figure 1 illustrates the elemental and macromolecular composition of the microalgae *M. salina*. The carbon content of dry *M. salina* biomass ($x_{C,X}$) grown under nutrient-replete conditions was measured to be 53%. This, as well as the overall elemental composition of the microalga determined in this work, were in accordance with the literature values (50–55% C in CDW) [28,29]. The ash content of 10.0% reported by Schädler et al. [12], which was used for calculations in this study, was also in the range of 4.2–11.7% as reported for

various algae species [30]. Based on its elemental composition, the molecular formula of *M. salina* biomass was determined to be $CH_{1.69}O_{0.39}N_{0.17}$.
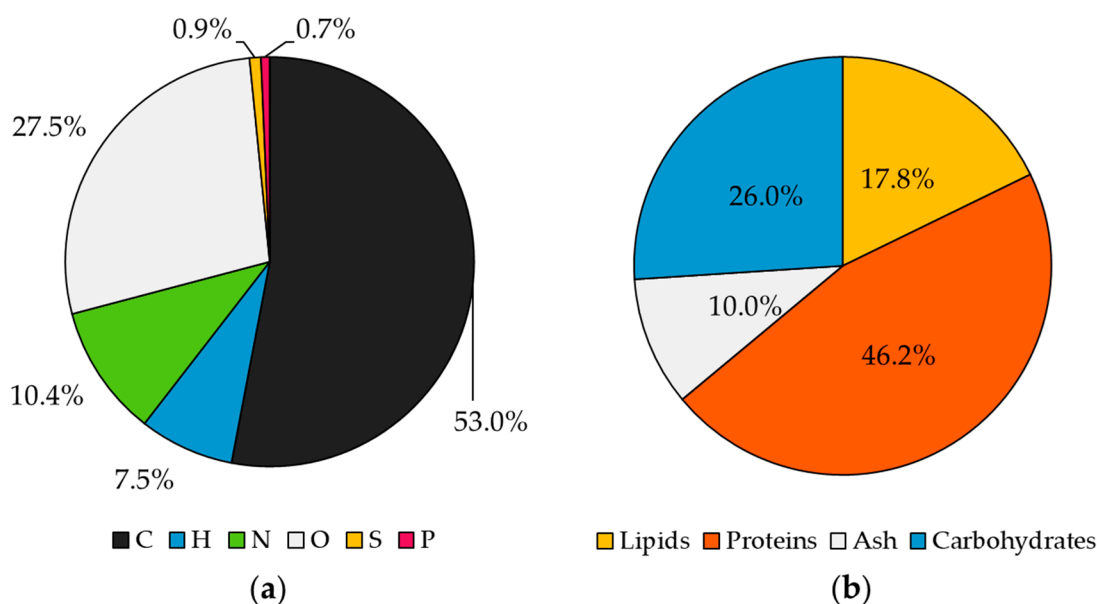

Figure 1. (**a**) Elemental and (**b**) macromolecular composition of *M. salina* biomass grown in nutrient-replete ASW medium. Ash content was assumed to be 10.0% based on previous reports [12].

Macromolecular analysis showed that the dry *M. salina* biomass contains 26% carbohydrates and 46% proteins, which indicates that around 68% of dry microalgae biomass could be utilized as a carbon source in a subsequent fermentation using microalgal biomass hydrolysate as feedstock. In the literature, a protein content between 30 and 60% of the dry biomass has been indicated for various microalgae species [26,29]. Toor et al. [29] measured 35% carbohydrates, 13% lipids, and 39% protein in the dry *M. salina* biomass when the remaining moisture content was excluded. However, the biomass they used was cultivated as a feedstock for biofuel production, most probably under nutrient-deplete conditions, which influences the macromolecular composition [12]. On the other hand, for *M. salina* grown under nutrient-replete conditions, Schädler et al. (2019) [12] reported 26% carbohydrates, 16% lipids, and 48% proteins in the dry mass of *M. salina*, which was remarkably similar to the macromolecular composition determined in this study.

3.2. Mechanical Cell Disruption

3.2.1. Ultrasonication

Figure 2 shows the disruption of *M. salina* biomass by ultrasonication. Microalgal biomass with a solids content ranging between 10 and 25% (*w/w*) was ultrasonicated for 40 min (Figure 2a). Cell disruption progressed very similarly for solids content between 10 and 20%, reaching nearly 40% after 40 min of ultrasonication. Only for a solids content of 25% did the degree of cell disruption reach 12% after 20 min and did not increase with further treatment. Typically, during ultrasonication, there is visible jet stream formation in the liquid medium, which also helps mix the sample. In this experiment, this was also the case for all the biomass samples except for the one with a 25% solids content, meaning that this sample was not mixed sufficiently during ultrasonication. Moreover, it was noted for biomass with a solids content of 25% that a dry biomass layer formed on the surface of the sonotrode, which grew thicker over time. Thus, it was concluded that ultrasonication is not suited for the cell disruption of microalgal biomass with such a high solids content and viscosity since the forces that accomplish cell disruption by ultrasonication act mainly through the liquid medium, which was not sufficiently present in this case.
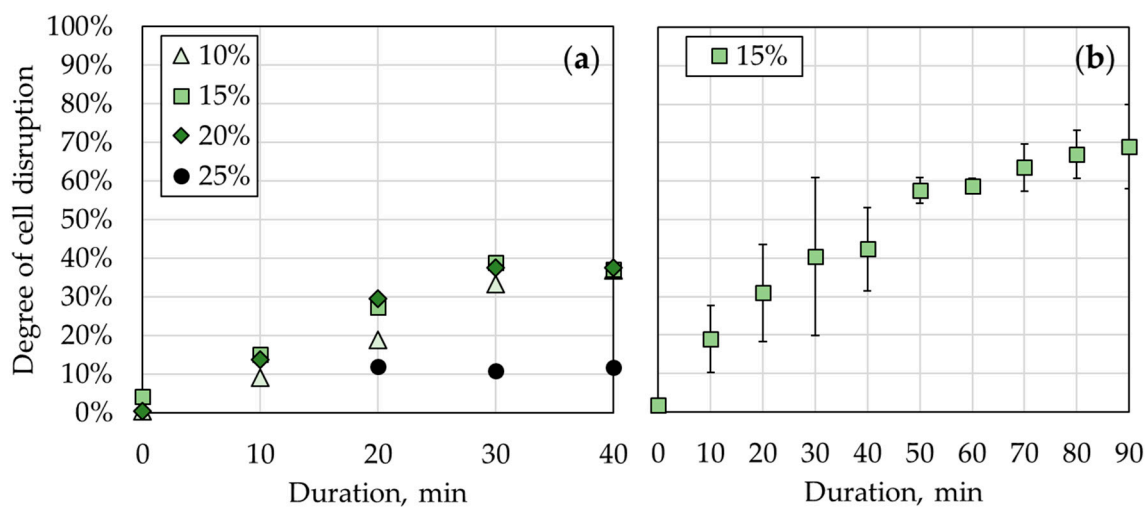
Figure 2. Disruption of *M. salina* biomass by ultrasonication. (**a**) Ultrasonication of microalgal biomass with various solids contents ranging between 10 and 25%, as the legend indicates, for 40 min; (**b**) ultrasonication of microalgal biomass with a 15% solids content for 90 min. Error bars show the standard deviation of triplicate experiments.

To determine if the disruption degree of *M. salina* cells would further increase with increasing ultrasonication time, a subsequent experiment with microalgal biomass with a 15% solids content was performed for a total treatment duration of 90 min (Figure 2b). It was shown that the cell disruption efficiency increased to 60% after 60 min and to 70% after 90 min of ultrasonication.

Yao et al. [31] examined the effect of high-intensity ultrasound on lipid extraction from high-solids viscous slurries of the *Microchloropsis* species. The extraction yields were similar with 12% and 20% solids content but decreased considerably for the 25% solids content of biomass. The same phenomenon was also observed in our study, confirming that there was an upper limit to the *M. salina* biomass density between 20% and 25% solids content, after which the efficiency of cell disruption via ultrasonication decreased drastically. On the other hand, the disruption degree achieved at different biomass concentrations below 20% was very similar. Yao et al. [31] suggested that such a decrease in efficiency could be due to an increased attenuation of ultrasound waves, which could result in less efficient cell rupture. This was attributed to the increase in the biomass viscosity and decrease in the speed of sound with the increasing solid content.

In this study, the highest disruption efficiency of *M. salina* cells achieved by ultrasonication was 70%, while 10–20% was reached after 10 min. This is in accordance with the literature values reported for ultrasonication at 20 kHz frequency for 10 min [32], whereas 60–90% disruption of the *Microchloropsis* species after 10–20 min has also been reported for ultrasonication at much higher frequencies (1.0–4.3 MHz) [32,33]. For the ultrasonic disruption of *Microchloropsis oculata* cells, Wang et al. [34] reported increased effectiveness by a combination of high-frequency focused ultrasound (3.2 MHz) and low-frequency non-focused ultrasound (20 kHz) treatments. However, frequencies applied at a large scale are usually lower due to concerns about energy consumption [35].

The literature regarding microalgal cell disruption using ultrasonication has focused more on the extraction efficiency of lipids or other products after the treatment, mostly without direct statements about the actual disruption efficiency. Nevertheless, its efficiency depends on microalgae species, biomass concentration, and operational conditions such as temperature, time, and frequency [18]. Ultrasonication of microalgae has been mainly applied as a pretreatment for biodiesel, bioethanol, and biogas production and has been shown to adequately break algal cells in low-density biomass suspensions, increasing the soluble fraction of organic matter, proteins, carbohydrates, and lipids [35]. On the other hand, for microalgal biomass hydrolysis, where the cell wall itself is the target rather than

an intracellular product to be released, ultrasonication on an industrial scale might be too energy- and time-intensive compared to other mechanical disruption methods, considering the high frequencies and treatment duration required for effective cell disintegration.

3.2.2. Bead Beating

Disruption of *M. salina* cells in a mixer mill was examined using beads of various materials and sizes. In this work, cell disruption experiments using a mixer mill were considered a preliminary exploration for a possible process transfer to an industrial-scale agitated media mill. Microalgal biomass with a solids content varying between 10 and 25% (*w/w*) was disrupted by bead milling for 40 min.

Figure 3 shows the cell disruption degree over time using beads with 0.5–1.0 mm diameters. The beads were made of zirconium oxide and agate, which had very similar densities of 6.0–7.0 g mL^{-1} (Table 2). As expected, the disruption efficiency increased with the declining biomass solids content and increasing milling time. The results were very similar for zirconium oxide and agate beads with the same diameter, which was to be expected since the densities of these two materials were quite similar.
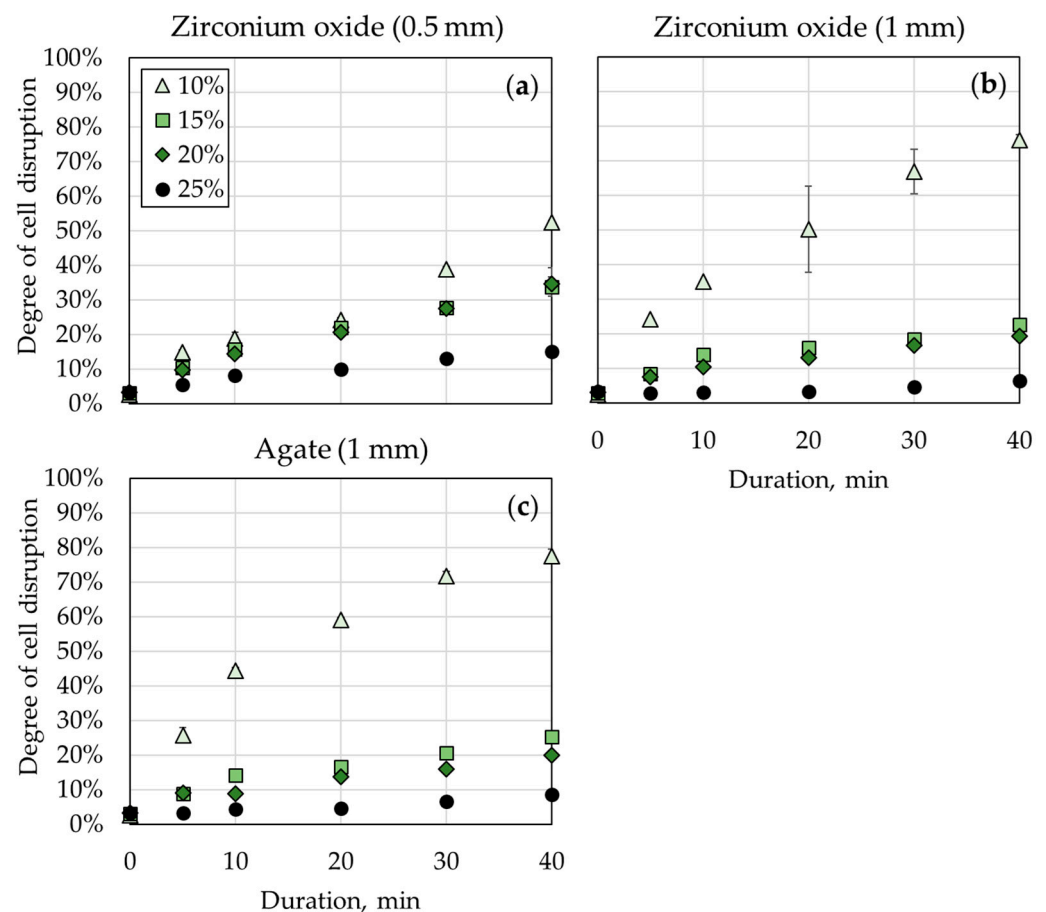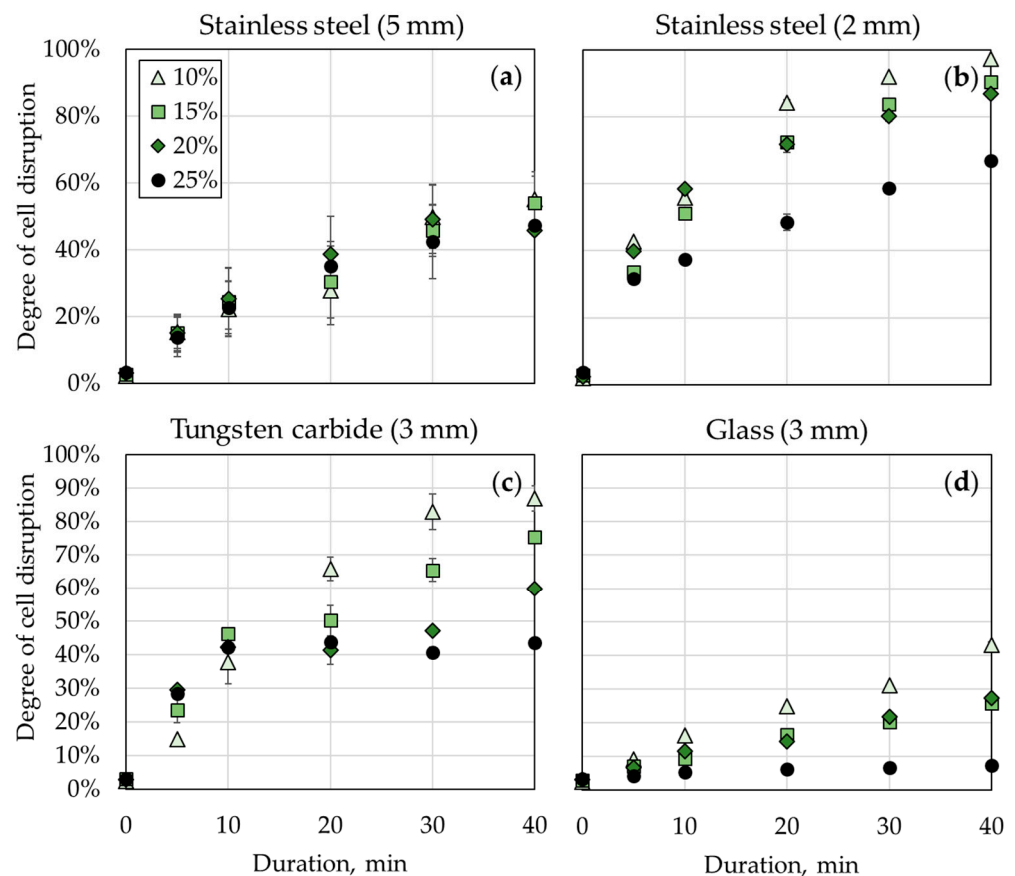

Figure 3. Disruption of *M. salina* biomass by bead milling using beads of various materials and sizes. Microalgal biomass with various solids content ranging between 10 and 25%, as indicated by the legend, was milled for 40 min. (**a**) Zirconium oxide (0.5 mm); (**b**) zirconium oxide (1.0 mm); (**c**) agate (1.0 mm). Error bars show the standard deviation of duplicate experiments.

For the disruption of microalgae, but also specifically of *Microchloropsis* species, by bead milling, a bead size of 0.3–0.6 mm has been reported to yield higher disruption efficiency than bead sizes over 1 mm [36–39]. This was also the case for biomass with solids content greater than 15% in this study, with the disruption efficiency being higher with a smaller bead size of 0.5 mm than with 1.0 mm, although it stayed below 35% in all cases.

However, on the contrary, for a solids content of 10%, the highest degree of disruption achieved with 0.5 mm beads was 53% after 40 min, which was around 25% lower than the 76–78% achieved after the same milling duration with 1 mm beads. This appears to be in contrast with the existing literature reports cited above.

Figure 4 shows the microalgal cell disruption using beads with a diameter between 2 and 5 mm. The beads were made of glass, stainless steel, and tungsten carbide, with material densities of 2.9 g mL^{-1}, 7.7 g mL^{-1}, and 15.0 g mL^{-1}, respectively. Using steel beads of 5 mm size, the disruption efficiency was almost independent of solids content and ranged between 46 and 54% for all biomass concentrations after 40 min. On the other hand, reducing the diameter of steel beads from 5 mm to 2 mm resulted in a remarkable increase in disruption degree. For biomass with a solids content of 10–20%, 87–97% of the cells were disrupted after 40 min. For a 25% solids content, only 67% of the cells were disrupted, which was still the highest disruption degree achieved with 25% solids content in this work. Using glass beads (3 mm) resulted in the lowest disruption efficiency of the dense *M. salina* biomass, as expected, due to its low density (Figure 4d). However, with tungsten carbide beads (3 mm), which had the highest density among the tested materials, a lower disruption efficiency than with the 2 mm steel beads was measured (Figure 4c).

Figure 4. Disruption of *M. salina* biomass by bead milling using beads of various materials and sizes. Microalgal biomass with various solids content ranging between 10 and 25%, as indicated by the legend, was milled for 40 min. (**a**) Stainless steel (5 mm); (**b**) stainless steel (2 mm); (**c**) tungsten carbide (3 mm); (**d**) glass (3.0 mm). Error bars show the standard deviation of duplicate experiments.

Very high sample temperatures and cell agglomeration with visible clumps were observed during cell disruption with tungsten carbide beads. This was probably the result of much higher energy input at the same mixing frequency compared to the other materials tested due to the significantly higher density of tungsten carbide. Hence, the measurements may have been faulty and lower than the actual values due to clumped cell debris being counted as intact cells. All in all, a higher material density of the same-sized beads was

determined to be more effective for disrupting the dense biomass of *M. salina*. To reduce the energy consumption of the cell disruption process, stainless steel should be preferred over tungsten carbide as a bead material since it allows sufficient disruption of the microalgal cells despite its much lower density. Furthermore, the best-performing beads proved to be the stainless-steel beads with a diameter of 2 mm, achieving the highest disruption efficiency for all biomass concentrations examined. Thus, the results indicate that the optimal bead size to disrupt dense microalgae biomass is around 2 mm.

The literature suggests that *Microchloropsis* species are harder to disrupt than most other microalgae species [16,37,40], and high bead material densities are more effective on microalgal cell disruption by bead milling [36,41]. For instance, Quesada-Salas et al. [37] used the same setup as Montalescot et al. [38] for the mechanical disruption of *Microchloropsis* species, with the only difference being the bead material, namely zirconium oxide instead of glass. This resulted in an increase of disruption efficiency by 40% compared to that reported by Montalescot et al. after one single pass.

For *Microchloropsis* biomass with 1% solids content, Quesada-Salas et al. [37] achieved 76–93% cell disruption after milling with zirconium oxide beads (0.4 mm) for 40 min. Pan et al. [39] reported 85% cell disruption for *Microchloropsis* species biomass with 15% solids after milling with zirconium oxide beads (0.8–1.0 mm) for 40 min. In this study, disruption efficiency achieved using the same bead size and material after the same milling duration was much lower. However, it must be noted that these studies used agitator bead mills (0.6–1.0 L grinding chamber), while in the current study, a mixer mill (20 mL grinding jars) was used, which is known to be less efficient than agitator mills [35]. Optimal bead size depends on agitator design and mill geometry and might vary for different bead mills [41]. In this study, the highest degree of disruption recorded for *M. salina* biomass with 10% solids was 97%, using 2 mm steel beads after 40 min of treatment. This corresponds to a theoretical maximum of 25.2 g L^{-1} final sugar concentration in the biomass hydrolysate, assuming that the sugar concentration achieved was proportional to the degree of cell disruption and 26% (*w*/*w*) carbohydrate fraction in the dry biomass. Even though increasing the initial solids content of the biomass to 20% would decrease the cell disruption efficiency to 87%, it would also increase the theoretical maximum sugar concentration of the hydrolysate to 45.2 g L^{-1}, which could be a better option considering the main objective of this work.

3.2.3. High-Pressure Homogenization

High-pressure homogenization for the disruption of *M. salina* cells was examined first on a laboratory scale using a bench-top HPH, followed by a scale-up to 200 L using an industrial HPH. On the laboratory scale, microalgal biomass with solids content varying between 10 and 25% was homogenized for up to 10 passes through the HPH. Figure 5 shows the results of cell disruption using the bench-top HPH at two different exit pressures. At a pressure of 1500 bar, for all CDW concentrations, disruption efficiency kept increasing with each pass through the HPH, reaching a final value between 40 and 63% after 10 passes (Figure 5a). At a pressure of 3000 bar, a higher disruption degree between 56 and 78% was achieved for all CDW concentrations after 10 passes (Figure 5b). However, the difference between various solids contents was more apparent at 3000 bar. With 10% solids content, a cell disruption degree of 75% was achieved already after four passes, while this took eight passes with a solids content of 15%. Still, disruption efficiency stayed below 80% in both cases despite further treatment. For biomass with 20–25% solids content, maximum disruption efficiency reached only 56–60%.
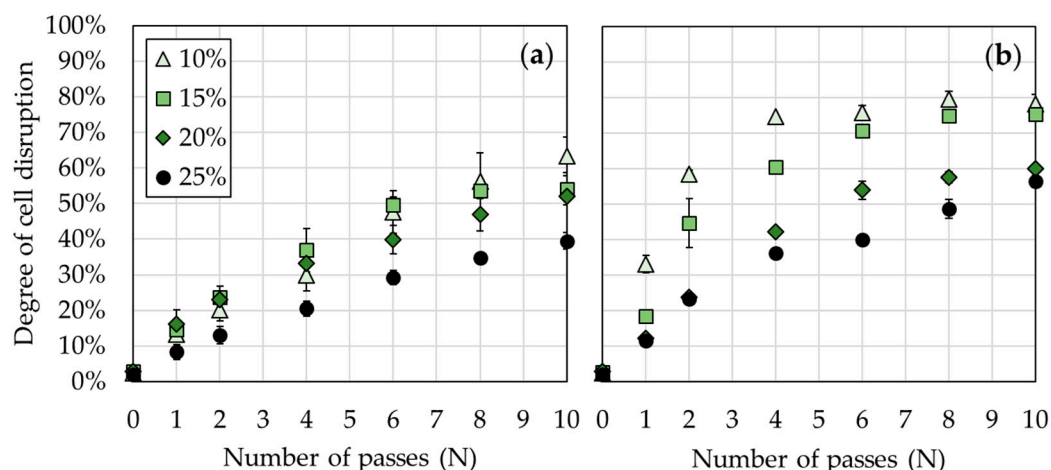
Figure 5. Disruption of *M. salina* biomass with HPH on a 200 mL scale. Microalgal biomass with various solids content ranging between 10 and 25%, as indicated by the legend, was homogenized for up to 10 passes. (**a**) Exit pressure of 1500 bar; (**b**) exit pressure of 3000 bar. Error bars show the standard deviation of triplicate experiments.

Figure 6 shows the results of the scale-up experiments to 200 L using an industrial HPH. Microalgal biomass with a solids content of 15% was homogenized with up to five passes at 1000 bar. The degree of cell disruption is plotted with respect to the number of equivalent passes, which is the time equivalent of a single pass when the biomass is circulated in an agitated tank during homogenization. On the 30 L scale, cell disruption efficiency reached 94% after 4.5 equivalent passes. In contrast, on 60 L and 200 L scales, cell disruption efficiency reached around 80% after 2–3 passes and did not increase afterward despite further homogenization. Nevertheless, the industrial HPH was more effective than the bench-top HPH, achieving over 70% cell disruption of biomass with 15% solids after two passes at 1000 bar, whereas this required six passes at 3000 bar with the bench-top HPH (Figures 5b and 6b).
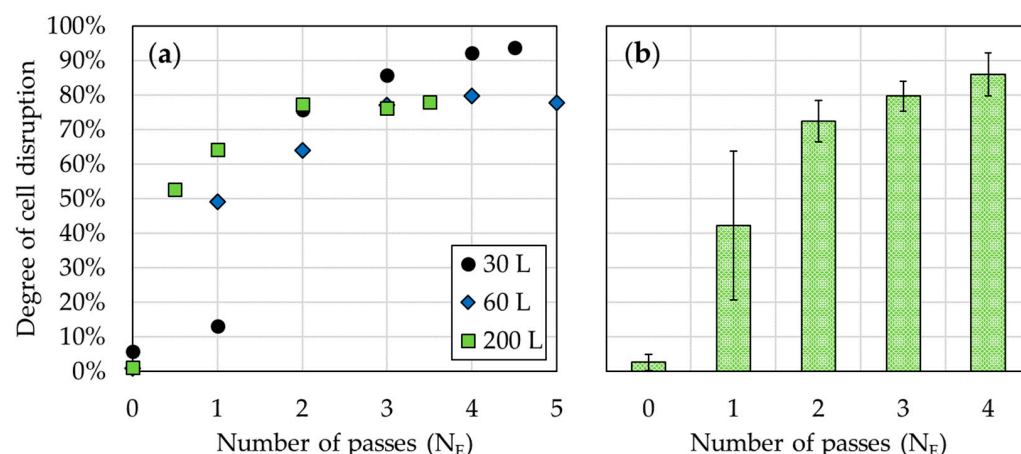
Figure 6. Disruption of *M. salina* biomass with HPH at 1000 bar exit pressure on 30 L (●), 60 L (◆), and 200 L (■) scales. Microalgal biomass with a solids content of 15% was homogenized for up to 5 passes. The degree of cell disruption is plotted with respect to the number of equivalent passes (N_E), which is the time equivalent of a single pass when the biomass is circulated in an agitated tank during homogenization. (**a**) Degree of cell disruption on different scales; (**b**) mean value of disruption degree on different scales. Error bars show the standard deviation between different experiments.

In this study, the industrial HPH proved more effective than the bench-top HPH, achieving a higher degree of cell disruption after fewer passes at a lower pressure. This is not surprising since the efficacy of HPH depends highly on the material and design of its

mechanical parts, especially of the homogenizing valve [19]. In general, HPH has proved to be an effective method for disrupting *M. salina* cells, even though the maximum disruption efficiency (86%) achieved with 15% solids content remained below the efficiency recorded for bead milling with 2 mm stainless-steel beads (90%).

The literature describes the best method of cell disruption as dependent on the microalgae strain. Halim et al. [42] stated that the most effective mechanical disruption method for *Chlorococcum* sp. cells is HPH, whereas Lee et al. [43] demonstrated that bead milling was significantly more efficient than HPH for disrupting *Botryococcus braunii* cells. At the same time, both agreed that ultrasonication was inefficient compared to these methods, as confirmed in this study, as well as others [18]. Grimi et al. [44] stated that HPH was the most effective disruption technique for extracting proteins from *Microchloropsis* species, but it also required the highest power consumption. Generally, a high solids content of the biomass to be processed helps reduce the specific energy consumption of both HPH and bead mills. However, contrary to the common view in the literature [18,45], the solids concentration of the microalgal biomass did influence the effectiveness of all mechanical cell disruption methods examined in this study. Hence, special caution is recommended when choosing a high biomass concentration above 15% dry weight for mechanical cell disruption.

Microalgal cell disruption using HPH has been examined mostly as a pretreatment method to improve the extraction yield of lipids or other intracellular products [36,44,46]. However, there are some quantitative data on the cell disruption of the *Microchloropsis* species using HPH. For the *Microchloropsis* species, a 67–100% cell disintegration degree has been reported using biomass with a low solids content below 1% and pressures up to 3000 bar [16,18]. Similar disintegration efficiencies of 56–94% were achieved in this study using high-density *M. salina* biomass with 10–25% solids. Additionally, 86% disruption efficiency was reproducibly achieved in this study using an industrial HPH on a pilot scale and with a high biomass density of 15% dry weight. This is considered to be a high disruption efficiency, considering that *Microchloropsis* species are known to have a very resistant and recalcitrant cell wall containing a layer of algaenan, which is a non-hydrolysable biopolymer [17], making them easier to cultivate under physically stressful conditions, while at the same time harder to disrupt compared to other species [16,35].

3.3. Chemical Hydrolysis of Undisrupted Cells

Since the mechanical disruption of microalgae cells requires high energy consumption, enzymatic hydrolysis of undisrupted *M. salina* cells with and without acid pretreatment was investigated first. Figure 7 shows the results of this experiment using the same enzyme dosing but with prior proteolysis (18 h) using proteases working at different pH optima of pH 3.5 and pH 7.0. The proteolysis was followed by autoclaving (at 121 °C for 20 min) at the specified pH for both sterilization and protease inactivation purposes. After autoclaving, the pH was adjusted to pH 5.0 for all batches, and the specified amounts of cellulase and mannanase mixtures were added for enzymatic hydrolysis (72 h). Since changes in reaction volume due to pH adjustments throughout the process were not negligible, sugar concentrations normalized to the initial reaction volume are presented in addition to the measured values.

After the proteolysis and heat pretreatment at pH 3.5, around 2.0 g L^{-1} glucose and 2.5–2.7 g L^{-1} mannose were already released, which corresponded to a saccharification efficiency of 13%. In contrast, no sugar release was observed for proteolysis and heat pretreatment at pH 7.0. Then, the same enzymatic hydrolysis procedure with polysaccharide-degrading enzymes was applied to all batches. For the batches that were pretreated at pH 3.5, final concentrations of 4.1–5.1 g L^{-1} glucose and 1.3–1.6 g L^{-1} mannose were achieved. On the other hand, for batches that were pretreated at pH 7.0, the final sugar concentrations were as low as 0.3–0.9 g L^{-1} glucose and 0.2–0.3 g L^{-1} mannose. Consequently, a significantly higher saccharification efficiency of 27–32% was achieved with acidic proteolysis and heat pretreatment combined with enzymatic hydrolysis, while it remained at 6–8% with proteolysis and heat pretreatment at a neutral pH.
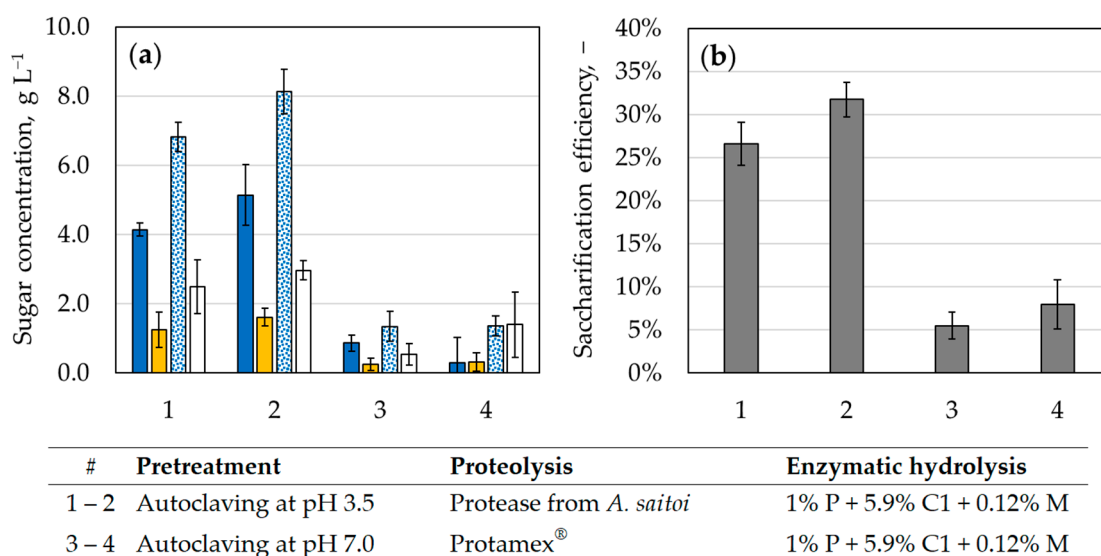
Figure 7. Chemical hydrolysis of undisrupted *M. salina* cells. Enzyme dosing is given as a mass ratio of CDW and adjusted to 1% protease (P), 5.9% cellulase (C1), and 0.12% mannanase (M) as indicated in the figure. Since changes in reaction volume due to pH adjustments throughout the process were not negligible, sugar concentrations normalized to the initial reaction volume are presented in addition to the measured values. (**a**) Actual and normalized final concentrations of glucose (■,▨) and mannose (■,□); (**b**) saccharification efficiency (η_{sac}). Error bars indicate the standard deviation of triplicate experiments.

Most studies on the hydrolysis of microalgal biomass have either focused on product extraction, such as lipid separation, or have utilized already-extracted biomass containing disrupted cells [47,48]. Some have reported over 90% carbohydrate solubilization of mechanically or chemically disrupted microalgae cells after enzymatic hydrolysis [10,11,49]. Direct enzymatic hydrolysis of undisrupted microalgae cells, especially with conclusions on biomass saccharification, is uncommon in the literature. Few studies focusing on enzymatic disruption of microalgal cell walls have used diluted biomass with 1–10% dry weight, which would yield a very diluted hydrolysate with around 2–20 g L^{-1} sugar [50]. In these studies, using cellulases or a combination of proteases and carbohydrases has accomplished saccharification yields of 47–96% with other microalgae species.

Saccharification efficiency of 27–32% achieved with acidic hydrolysis followed by enzymatic hydrolysis was relatively low compared to literature reports for other microalgae strains mentioned above. Scholz et al. [17] determined that the cell wall of *M. gaditana* contained around 14% algaenan, which is a non-hydrolysable biopolymer, presenting itself as an insoluble residue following severe acid and base hydrolysis, that is also well established in other species of *Microchloropsis*, including *M. salina* [51]. Thus, a relatively low saccharification efficiency is to be expected with *Microchloropsis* species even after chemical hydrolysis.

Hernández et al. [6] carried out a comparable study regarding saccharification of undisrupted *M. gaditana* biomass with acidic hydrolysis followed by enzymatic treatment. They reported that 93 mg sugars per g dry weight (DW) were released after diluting the biomass with 7% (*v/v*) sulfuric acid and autoclaving (at 121 °C for 30 min). In this study, proteolysis and heat pretreatment at pH 3.5 (autoclaving at 121 °C for 20 min) released only 27–29 mg g^{-1} DW sugars. They also noted that alkaline pretreatment (5 M NaOH, 90 °C for 30 min) of the biomass had a sugar release yield of 14 mg g^{-1} DW, which was lower than with acidic hydrolysis. Furthermore, Hernández et al. [6] demonstrated that acidic hydrolysis improved the efficacy of subsequent enzymatic hydrolysis with cellulases significantly, with an increase of sugar release from 15 mg g^{-1} DW to 129 mg g^{-1} DW. In the current study, even though this effect was confirmed, the influence of acidic hydrolysis

prior to enzymatic hydrolysis was less remarkable with an increase of sugar release from 12–17 mg g^{-1} DW to merely 57–68 mg g^{-1} DW. This difference might have originated from using *M. salina* cells grown in a nutrient-replete medium since these have a different macromolecular and cell wall composition [12], which could have resulted in the increased structural stability of the cell wall and made it harder to disrupt or hydrolyze.

Although acidic hydrolysis of *M. salina* biomass improved the saccharification yield, it should be noted that it also resulted in a substantial dilution of the biomass due to the addition of acid and base to adjust the pH of the reaction medium. More precisely, dilution of the biomass by a factor of 1.3–1.6 resulted in a decrease of final glucose concentration from 6.8–8.1 g L^{-1} to 4.1–5.1 g L^{-1}. Moreover, the excessive addition of acid and base resulted in an increase in the salt content of the hydrolysate, which may have negatively affected microbial growth when it was used as a feedstock for fermentation. Hence, the acidic hydrolysis approach was avoided in further hydrolysis experiments in this work.

3.4. Enzymatic Hydrolysis of Disrupted Cells

Enzymatic hydrolysis of mechanically disrupted *M. salina* cells was first investigated on a milliliter scale. Initially, the effects of the sterilization method and degree of cell disruption on the effectiveness of enzymatic hydrolysis were investigated, considering the impact on a subsequent scale-up. Then, the dosing of various enzymes was examined for increased saccharification efficiency, and the hydrolysis was scaled up to 200 L using the best-performing enzyme composition.

Table 7 presents the experimental results for the enzymatic hydrolysis of mechanically disrupted *M. salina* cells, showing the disruption degree of microalgal biomass prior to enzymatic hydrolysis, enzyme dosing used, the concentration of glucose and mannose released, and the saccharification efficiency achieved in experiments on a milliliter scale.

First of all, the influence of the sterilization method and cell disruption degree on subsequent enzymatic hydrolysis of mechanically disrupted *M. salina* cells was examined. As a sterilization method, autoclaving at 121 °C for 20 min was compared with the addition of antibiotics (each 100 mg L^{-1} of kanamycin and tetracycline) to inhibit the growth of contaminants. These are labeled in Table 7 as experiments number 1 and 2, respectively. It was demonstrated that skipping the autoclaving step and using antibiotics instead did not affect hydrolysis efficiency, which reached 10% in both cases. Therefore, the addition of antibiotics was preferred to prevent contamination effects on biomass hydrolysis in the following experiments.

The degree of cell disruption had a significant influence on the effectiveness of hydrolysis. An increase in initial cell disintegration degree from 70% to 92% increased saccharification efficiency from 10% to 16%. As anticipated, higher degrees of mechanical cell disruption at the beginning of enzymatic hydrolysis resulted in a higher hydrolysis efficiency since the carbohydrates in the cell wall become more exposed, making them more readily available for the enzymes.

The effects of adding hemicellulase or protease to the enzyme mixture on hydrolysis efficiency were also investigated. Adding 1% hemicellulase to the enzyme mixture in addition to cellulase and mannanase improved biomass hydrolysis minimally, increasing the saccharification efficiency by 2% from 16% to 18%. Adding 1% protease to the enzyme mixture in addition to cellulase and mannanase increased hydrolysis efficiency only by 1% to 11%. Thus, the use of hemicellulase or protease in addition to the carbohydrases affected the effectiveness of enzymatic hydrolysis only negligibly, in contrast to the literature reports for other microalgae strains [50], and was therefore omitted in the following experiments.

Next, two different cellulase mixes, namely Cellic® CTec3 HS and Rohament® CEP, labeled as C1 and C2 in Table 7, respectively, were compared with respect to the saccharification efficiency. Only 2% of the carbohydrates were solubilized using a mannanase dose of 0.12% without cellulases. Using 5% Cellic® CTec3 HS in addition to mannanase improved the saccharification efficiency to 10%, whereas with 5% Rohament® CEP, it increased to 12%. With Cellic® CTec3 HS, more mannose was released, while Rohament® CEP solubilized

more glucose. Due to its better performance than Cellic® CTec3 HS, as well as its easy-to-use powder form, Rohament® CEP was used in further enzymatic hydrolysis experiments.

Table 7. Enzymatic hydrolysis of mechanically disrupted *M. salina* cells on a milliliter scale. Disruption degree of microalgal biomass prior to enzymatic hydrolysis, as well as the enzyme type and dosing (g enzyme per g CDW) used, are listed for each experiment. Names of the enzymes used are abbreviated. C1: Cellic® CTec3 HS; C2: Rohament® CEP; M: Rohalase® GMP; H: Hemicellulase from *A. niger*; P: Protamex®. CDW concentration of the initial biomass prior to mechanical cell disruption was 150 g L^{-1} in all cases. Concentrations of glucose and mannose measured after the enzymatic hydrolysis were assumed to be representative of all sugars released and used as basis for the calculation of the saccharification efficiency.
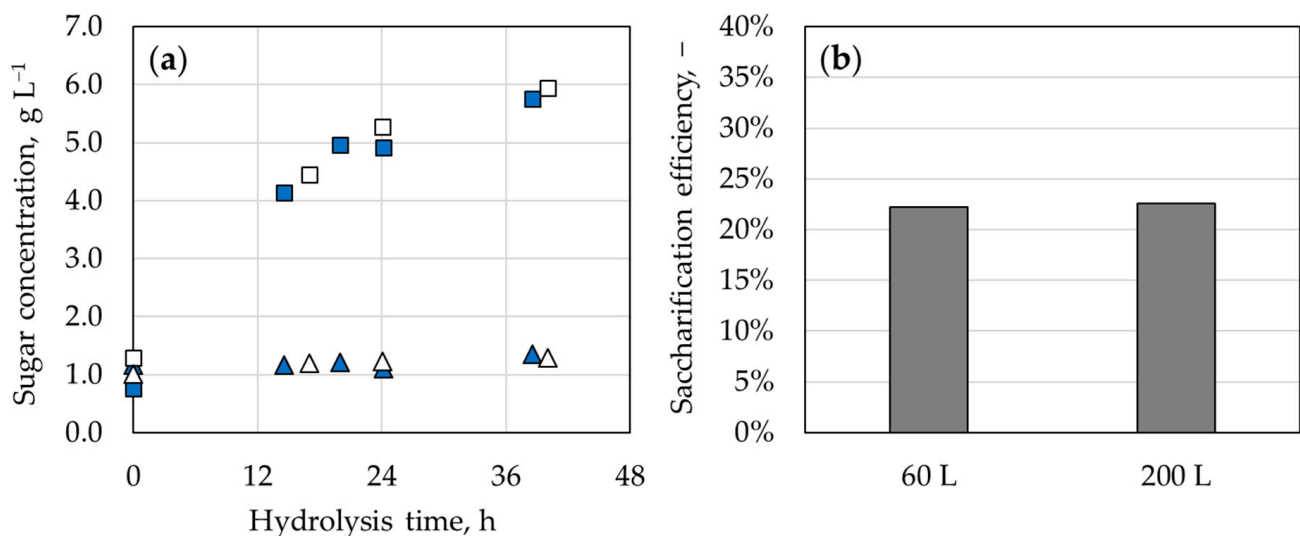
Experiment #	Degree of Cell Disruption, −	C1, g g^{-1}	C2, g g^{-1}	M, g g^{-1}	H, g g^{-1}	P, g g^{-1}	Glucose, g L^{-1}	Mannose, g L^{-1}	Saccharification Efficiency, −
Effect of autoclaving vs. antibiotic usage for sterilization									
1	75%	5.92%	–	0.12%	–	–	2.63 (±0.10)	1.88 (±0.38)	10.1% (±0.9%)
2	75%	5.92%	–	0.12%	–	–	2.45 (±0.08)	2.05 (±0.05)	10.1% (±0.2%)
Effect of cell disruption degree									
3	70%	5.92%	–	0.12%	–	–	1.93 (±0.15)	0.93 (±0.07)	10.2% (±0.6%)
2	75%	5.92%	–	0.12%	–	–	2.45 (±0.08)	2.05 (±0.05)	10.1% (±0.2%)
4	92%	5.92%	–	0.12%	–	–	3.25 (±0.08)	0.93 (±0.09)	16.4% (±0.3%)
Addition of hemicellulase (H) and protease (P)									
4	92%	5.92%	–	0.12%	0.00%	–	3.25 (±0.08)	0.93 (±0.09)	16.4% (±0.3%)
5	92%	5.92%	–	0.12%	1.00%	–	3.67 (±0.12)	0.91 (±0.19)	18.0% (±0.5%)
2	75%	5.92%	–	0.12%	–	0.0%	2.45 (±0.08)	2.05 (±0.05)	10.1% (±0.2%)
6	75%	5.92%	–	0.12%	–	1.0%	2.68 (±0.32)	2.22 (±0.18)	11.0% (±0.8%)
Comparison of cellulase mixes Cellic® CTec3 HS (C1) vs. Rohament® CEP (C2)									
7	70%	0.0%	0.0%	0.00%	–	–	0.35 (±0.01)	0.22 (±0.00)	2.0% (±0.0%)
3	70%	5.92%	0.0%	0.12%	–	–	1.93 (±0.15)	0.93 (±0.07)	10.2% (±0.6%)
8	70%	0.0%	5.0%	0.12%	–	–	2.83 (±0.10)	0.47 (±0.06)	11.8% (±0.4%)
Variation of cellulase (C2) dosing									
7	70%	–	0.0%	0.00%	–	–	0.35 (±0.01)	0.22 (±0.00)	2.0% (±0.0%)
8	70%	–	5.0%	0.12%	–	–	2.83 (±0.10)	0.47 (±0.06)	11.8% (±0.4%)
9	70%	–	10.0%	0.12%	–	–	4.58 (±0.02)	0.47 (±0.02)	18.1% (±0.1%)
10	78%	–	0.0%	0.00%	–	–	1.48 (±0.02)	0.89 (±0.01)	8.6% (±0.1%)
11	78%	–	10.0%	0.12%	–	–	5.54 (±0.30)	1.31 (±0.08)	24.8% (±1.1%)
12	78%	–	15.0%	0.12%	–	–	5.94 (±0.56)	1.29 (±0.03)	26.1% (±2.0%)
Variation of mannanase (M) dosing									
10	78%	–	0.0%	0.00%	–	–	1.48 (±0.02)	0.89 (±0.01)	8.6% (±0.1%)
11	78%	–	10.0%	0.12%	–	–	5.54 (±0.30)	1.31 (±0.08)	24.8% (±1.1%)
13	78%	–	10.0%	2.00%	–	–	6.90 (±0.73)	1.30 (±0.14)	29.6% (±2.7%)

Then, the effect of cellulase dosing on saccharification efficiency was examined. For this, two sets of experiments with different initial cell disruption degrees are presented in Table 7. In the case of biomass with a 70% cell disruption degree, using 5% and 10% cellulase in addition to mannanase increased saccharification efficiency by 10% and 16%, respectively. Using biomass with a 78% cell disruption degree, dosing of 10% and 15% cellulase in addition to mannanase resulted in an efficiency increase of 16% and 18%, respectively. Here, although the best results of 7.2 g L^{-1} sugars (glucose and mannose) and 26% saccharification efficiency were reached with 15% cellulase dosing, the difference from 10% cellulase was not significant enough to consider it better with respect to price-

performance ratio. For hydrolysis of the biomass with a 78% cell disruption degree, adding 10% cellulase together with 0.12% mannanase yielded 6.9 g L^{-1} sugars released and 25% saccharification efficiency. Thus, a cellulase dose of 10% was used in the enzyme mixture in further hydrolysis experiments.

Table 7 also reveals the results of the experiment investigating the effect of mannanase dosing on saccharification efficiency. Using 10% cellulase only without mannanase, 9% of the carbohydrates of the microalgal biomass were solubilized. Adding 0.12% mannanase into the enzyme mixture increased the hydrolysis efficiency to 25%, and a further increase of mannanase dosing to 2.0% increased the efficiency further to 30%. Moreover, the sum of glucose and mannose released increased from 2.4 g L^{-1} to 6.9 g L^{-1} and further to 8.2 g L^{-1}, respectively. This indicates a possible synergy between the cellulase and mannanase mixes used, which led to improved glucose release with increased dosing of mannanase, even though the amount of mannose released remained the same.

Scale-up of the enzymatic hydrolysis of mechanically disrupted *M. salina* biomass to first 60 L, and, finally, to 200 L, was performed successfully. Figure 8 shows the results of the scale-up experiments. On both scales, a cellulase dosing of 10% of CDW was applied. Even though a higher mannanase dose (1.0%) was used on the 200 L scale, no improvement in saccharification efficiency was observed compared to the 60 L scale with 0.12% mannanase dosing. The final concentration of released glucose was 5.7–5.9 g L^{-1}, whereas 1.3–1.4 g L^{-1} mannose was solubilized. Hence, the resulting saccharification efficiency was very similar, namely 22.2% and 22.6% in the 60 L and the 200 L scale processes, respectively. Nonetheless, saccharification efficiency achieved on the 200 L scale was 7% lower than the 30% recorded on the milliliter scale.

Scale	Cell disruption	Enzymatic hydrolysis
60 L	78%	10% C2 + 0.12% M
200 L	78%	10% C2 + 1% M

Figure 8. Enzymatic hydrolysis of mechanically disrupted *M. salina* cells on 60 L (blue) and 200 L (white) scales. The degree of cell disruption was 78% in both experiments. Enzyme dosing is given as a mass ratio of CDW and adjusted to 10.0% cellulase (C2) and 0.12% or 1.00% mannanase (M) for hydrolysis on the 60 L, and the 200 L scales, respectively. (**a**) Final concentrations of glucose (■) and mannose (▲) on the 60 L scale and glucose (□) and mannose (△) on the 200 L scale; (**b**) saccharification efficiency (η_{sac}).

Based on the sugar composition of *M. salina* grown in a nutrient-replete medium in thin-layer cascade photobioreactors as reported by Schädler et al. [12], with an initial

CDW concentration of 250 g L^{-1} and 100% saccharification efficiency, the resulting microalgae hydrolysate would have a 53.4 g L^{-1} total concentration of glucose and mannose. However, the technical equipment used in the current study allowed for the processing of only 150 g L^{-1} CDW containing microalgal biomass since the industrial HPH used for mechanical cell disruption did not allow for higher feed stream viscosity ($\leq$20 mPa s at a shear rate of 1000 s^{-1}). Hence, calculating with an initial CDW concentration of 150 g L^{-1} and 100% saccharification efficiency, the resulting microalgae hydrolysate would have a 32.1 g L^{-1} total concentration of glucose and mannose. Nevertheless, the best results obtained in this experimental series were 8.2 g L^{-1} on a milliliter scale and 7.2 g L^{-1} on a 200 L scale.

In this work, the maximum saccharification efficiency achieved was 30%, which corresponds to 77.3 mg released sugars per g CDW, very similar to the yield reported by Mirsiaghi and Reardon [52] using commercial enzyme mixtures on disrupted *M. salina* biomass. Nevertheless, a 30% saccharification yield is way below the expected range of 47–90% [50], yielding lower sugar concentrations than what would be required for the use of the hydrolysate as a feedstock for fermentation. One solution to the unexpectedly low sugar content of the microalgae biomass hydrolysate would be concentrating the hydrolysate using an evaporator, which was not demonstrated in this study due to the lack of appropriate equipment for a large-scale application.

It might be possible to improve the carbohydrate saccharification yield for high-density *M. salina* biomass by adding other commercially available enzymes with various activities into the enzyme cocktail used. With the help of a growth inhibition screen, Gerken et al. [53] suggested that chitinase, lysozyme, pectinase, sulfatase, b-glucuronidase, and laminarinase could aid the enzymatic cell wall degradation of *Microchloropsis* strains. Moreover, Horst et al. [54] could improve the lipid extraction yield for autoclaved *M. oculata* biomass by around 20% using Viscozyme (a multi-enzyme mixture containing a wide range of carbohydratases) and Proteinase K (an alkaline serine protease of fungal origin). However, the prospects of success at improving the effectiveness of enzymatic hydrolysis seem to be low with *M. salina* cells grown in nutrient-replete medium, since these have a different macromolecular and cell wall composition [12,55] and are apparently harder to disrupt and hydrolyze than the *M. salina* cells grown in nutrient-limited medium [55,56]. Applying nutrient limitation on the microalgae culture, on the other hand, would reduce biomass productivity.

3.5. Phosphorus Elimination

3.5.1. Preliminary Precipitation Experiments Using Phosphate Buffer

Preliminary experiments on phosphate precipitation were carried out using a phosphate buffer and FeCl$_3$ as the precipitating agent at a pH range of pH 4.5–5.5. Various ratios of iron to phosphorus were examined, adding different amounts of concentrated FeCl$_3$ solution to the buffer.

As seen in Figure 9, using an Fe:P stoichiometric ratio of 1:1 resulted in a reduction of phosphate concentration from 164 mg L^{-1} to 51 mg L^{-1}, yielding a phosphate depletion of 69%. On the other hand, an Fe:P ratio of 1.5:1 and 2:1 reduced the phosphate concentration to 6 mg L^{-1} and 1 mg L^{-1}, achieving 96% and 99% phosphate depletion, respectively. Another experiment showed that the centrifugation duration did not have a noticeable influence on the efficiency of phosphate precipitation (see Figure S1), which is practical for large-scale processing of biomass hydrolysate since no settling time is required during continuous centrifugation of the hydrolysate.
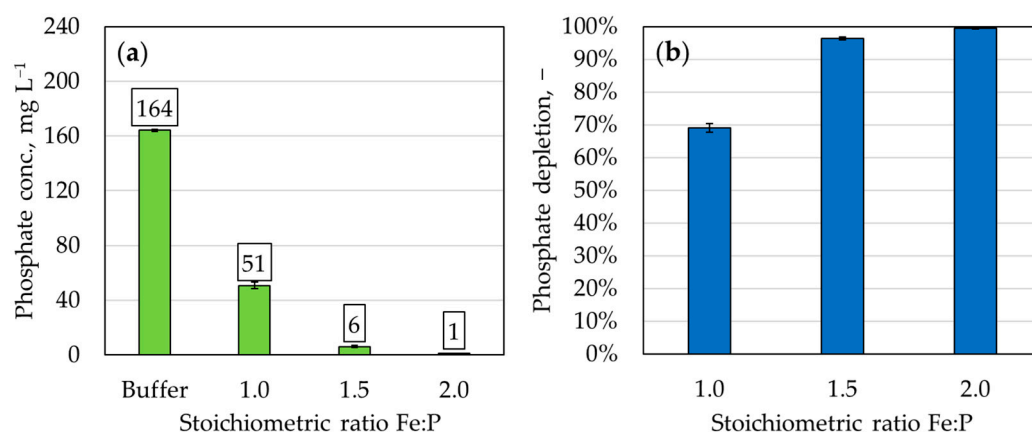
Figure 9. Variation of the Fe:P stoichiometric ratio for phosphate precipitation of a phosphate buffer using FeCl$_3$. (**a**) Phosphate concentration in the buffer solution and after precipitation with various Fe:P ratios; (**b**) degree of phosphate depletion with various Fe:P ratios.

3.5.2. Phosphate Precipitation Using Microalgae Hydrolysate

Initial experiments with microalgae hydrolysate showed that a single-step process was not as effective as demonstrated with the phosphate buffer (see Table S1). Moreover, a single-step precipitation with a stoichiometric excess of iron over phosphorus would require uneconomically large amounts of FeCl$_3$. Hence, a stepwise reduction of the phosphorus level was developed. To prevent an unnecessary dilution of the hydrolysate, the precipitating agent FeCl$_3 \cdot 6\,H_2O$ and KOH for pH adjustment were added to the reaction mixture in solid form.

Phosphate precipitation of the microalgal biomass hydrolysate was carried out on a 200 L scale. An Fe:P stoichiometric ratio of 1.2:1 was used in the first step, which was increased to 2:1 for the second step. As shown in Table 8, the initial phosphate concentration in the microalgae hydrolysate was 6.5 g L^{-1}, which was much higher than the concentration anticipated based on the elemental composition of *M. salina* biomass (2−3 g L^{-1}). Nonetheless, the phosphate content was successfully reduced to 83 mg L^{-1} and then to 28 mg L^{-1} after each step, with an overall phosphate depletion degree of 99.6%. Performing additional precipitation steps on a milliliter scale allowed a decrease of the phosphate concentration to around 25 mg L^{-1}, but not further (see Tables S1 and S2).

Table 8. Stepwise phosphate precipitation of microalgae hydrolysate on a 200 L scale. An Fe:P stoichiometric ratio of 1.2 and 2.0 was used in 1st and 2nd steps, respectively. The reaction mixture was centrifuged using a disc separator after each step. Precipitating agent FeCl$_3 \cdot 6\,H_2O$ and KOH for pH adjustment were added to the reaction mixture in solid form to prevent an unnecessary dilution of the hydrolysate.

	Fe:P Ratio	Phosphate Concentration, mg L^{-1}	Phosphate Depletion, %
Hydrolysate	—	6512.0	—
Step 1	1.2	82.6	98.7
Step 2	2.0	27.6	66.6
Final	—	27.6	99.6

In general, phosphorus limitation of microbial growth requires a very high C/P ratio around 3000–4000 g g^{-1} to be present in the cultivation medium [5,10]. To achieve this C/P ratio with a phosphate concentration of 25–100 mg L^{-1}, a sugar content of 61–326 g L^{-1} would be required, which is significantly higher than the concentrations achieved in the biomass hydrolysate in this study.

An alternative strategy would be to first concentrate the biomass hydrolysate to increase the sugar concentration, for instance, by evaporation, and then perform the

phosphorus elimination. In this way, the increased sugar concentration would make it possible to reach a higher C/P ratio at the same phosphate level.

Using a very similar procedure with a Fe:P ratio of 1.5:1 on a different microalgae hydrolysate, Meo et al. [10] successfully reduced the phosphate content of a microalgae hydrolysate by 99.7% from 1.62 g L^{-1} to 10 mg L^{-1}. However, the biomass they used was pretreated in a different manner, which resulted in a much lower organics concentration in the biomass hydrolysate. Takács et al. [24] suggested that there might be various reasons making it hard to achieve very low phosphorus levels in streams containing high amounts of organic matter, such as the formation of organic side products with Fe^{3+} and other components, most importantly, charged organics (through ion-pairing and binding), also stating that the extent of these reactions is unknown. Furthermore, soluble ferric–phosphate and ferric–hydroxide complexes might form, which hinders the conversion of soluble phosphorus to the particulate form by binding up Fe^{3+} or PO_4^{3-} ions in soluble complexes.

Phosphorus elimination of the microalgal biomass hydrolysate using $FeCl_3$ generates significant amounts of precipitated $FePO_4$. Ferric–phosphate has potential applications in various industries, including its use in anti-corrosion coatings in the steel industry, as a cathode material for Li-ion batteries, and in chemical waste immobilization [57]. Since phosphate is a valuable nutrient, the production of fertilizers using ferric–phosphate is also an extensively researched topic. The potential uses of the $FePO_4$ precipitated from biomass hydrolysate depends, however, on the size and morphology of the iron phosphate crystals formed [57].

3.6. Composition of the Microalgal Biomass Hydrolysate

Table 9 shows the sugar composition, as well as the phosphate and protein concentrations, of the microalgae hydrolysate produced on the 200 L scale after phosphate precipitation. Based on the sugar composition of *M. salina* grown in a nutrient-replete medium [12], microalgae biomass with a CDW concentration of 150 g L^{-1} contained 24.2 g L^{-1} glucose, 7.5 g L^{-1} mannose, 2.6 g L^{-1} galactose, and 1.9 g L^{-1} rhamnose, with the remaining carbohydrates amounting to 2.4 g L^{-1}. According to these values, only 15.2% of mannose could be solubilized with the applied hydrolysis protocol, whereas 58.5% saccharification efficiency of galactose was achieved. Nevertheless, considering an overall saccharification efficiency of 23%, sugar concentrations measured in the final microalgae hydrolysate are in accordance with these values.

Table 9. Measured sugar composition, protein content, and phosphate concentration of the *M. salina* biomass hydrolysate.

Component	Concentration, g L^{-1}	Mass Fraction in Total Sugars, %
Glucose	5.32	65.9
Mannose	1.14	14.1
Galactose	1.52	18.8
Rhamnose	0.08	1.0
Xylose	0.02	0.2
Total sugars	8.08	100.0
Phosphate	2.44	–
Total protein and peptide	13.4	–

Meo et al. [10] reported 40.8 g L^{-1} glucose, 2.0 g L^{-1} mannose, 4.3 g L^{-1} galactose, and 13.3 g L^{-1} protein in the microalgae hydrolysate of *Scenedesmus* species starting with a CDW concentration of 250 g L^{-1}. Even though the total sugar concentration achieved by Meo et al. [10] was much higher, the protein content was very similar to the concentration measured in this work. The amino acid concentration of the hydrolysate was not analyzed since the proteases used for biomass hydrolysis in this study were endopeptidases, which cannot break down peptides into their monomers. Considering the macromolecular com-

position of the dry *M. salina* biomass, the measured 13.4 g L^{-1} concentration of protein and peptide in the hydrolysate corresponds to 19.3% protein solubilization by hydrolysis of the initial biomass with 150 g L^{-1} CDW concentration.

The elemental composition of the microalgae hydrolysate after final processing is presented in Table 10. Based on these values, the microalgae hydrolysate produced contained 27.4 g L^{-1} carbon, 16.6 g L^{-1} nitrogen, and 0.8 g L^{-1} phosphorus. This corresponds to a C/N ratio of 1.65 g g^{-1} and a C/P ratio of 34.4 g g^{-1}. For comparison, yeast biomass grown without nutrient limitation has a C/N ratio of 5.37 g g^{-1} and a C/P ratio of 55.4 g g^{-1} [5], and synthetic media typically used for fermentation processes require similar amounts of these nutrients with respect to the carbon supplied [1,58,59]. Hence, these results suggest that the microalgal biomass hydrolysate could be used as a cultivation medium without any need for additional nitrogen or phosphorus supplementation.

Table 10. Elemental composition of the *M. salina* biomass hydrolysate.

Hydrolysate	Mass Fraction of the Element, %					Ratio, g g^{-1}	
	C	H	N	S	P	C/N	C/P
After hydrolysis	2.76	9.90	1.67	0.00	0.08	1.65	34.4
After P elimination	2.52	10.84	1.65	0.00	0.00	1.53	2100.0

After phosphorus elimination, the C/P ratio became 2100 g g^{-1}. However, it should be noted that the C/P ratio was so high due to the high protein and peptide content despite the low sugar concentration. Assuming that sugars would be the only carbon source utilized by the microorganisms in a subsequent fermentation, the C/P ratio of the hydrolysate would be only 268 g g^{-1}.

The mass fraction of carbon in the produced microalgae hydrolysate was determined to be 2.52%. This information allows for the calculation of the carbon solubilization efficiency as a measure of the overall hydrolysis efficiency. According to the total sugars measured in the hydrolysate (8.08 g L^{-1}) and the carbon content of the dry microalgae biomass, a saccharification efficiency of 21% and a carbon solubilization efficiency of 31% were achieved on a 200 L scale in this study. Since microorganisms can utilize both sugars and peptides as carbon sources, total carbon solubilization is more important for the use of biomass hydrolysate as a feedstock for fermentation and should be considered as a more practical measure of hydrolysis efficiency in this case.

4. Conclusions

The aim of this study was to investigate the potential of *M. salina* biomass as a feedstock for fermentation by examining various cell disruption and hydrolysis methods. For the marine microalgae *M. salina*, the most effective cell disruption method was determined to be bead milling with 2 mm stainless-steel beads. Despite the high degree of cell disruption, enzymatic hydrolysis of the microalgal biomass yielded a saccharification efficiency of around 20–25%. Even though the sugar concentration of the resulting hydrolysate was low for a fermentation medium (<10 g L^{-1}), it would be possible to concentrate the hydrolysate by evaporation, for example, using a thin-film evaporator, to achieve higher sugar concentrations.

Elemental analysis of the *M. salina* biomass hydrolysate showed that the microalgae hydrolysate could be used as a cultivation medium without any need for additional nitrogen or phosphorus supplementation. The hydrolysate produced was rich in phosphates as well as nitrogen due to a high content of proteins and peptides. The use of microalgal biomass hydrolysate in fermentation processes requiring phosphorus limitation was also shown to be feasible through phosphorus depletion using FeCl$_3$ as a precipitating agent.

All in all, this study presents useful insights into the disruption and enzymatic hydrolysis of marine microalgae species, as well as their potential as a feedstock for fermentation. However, the low-carbohydrate saccharification yield achieved with *M. salina* makes it a

poor choice for use as feedstock. Alternatively, other microalgae strains that are richer in carbohydrates and easier to disrupt, such as the members of *Porphyridium* and *Scenedesmus* genera [40,60], could be preferred. This would decrease the cost of the energy-intensive mechanical cell disruption and allow for more efficient biomass hydrolysis and, thus, for a higher sugar concentration in the resulting microalgal biomass hydrolysate.

References

1. Mittermeier, F.; Fischer, F.; Hauke, S.; Hirschmann, P.; Weuster-Botz, D. Valorization of wheat bran by co-cultivation of fungi with integrated hydrolysis to provide sugars and animal feed. *BioTech* **2024**, *13*, 15. [CrossRef] [PubMed]
2. Knesebeck, M.; Schäfer, D.; Schmitz, K.; Rüllke, M.; Benz, J.P.; Weuster-Botz, D. Enzymatic one-pot hydrolysis of extracted sugar beet press pulp after solid-state fermentation with an engineered *Aspergillus niger* strain. *Fermentation* **2023**, *9*, 582. [CrossRef]
3. Schäfer, D.; Schmitz, K.; Weuster-Botz, D.; Benz, J.P. Comparative evaluation of *Aspergillus niger* strains for endogenous pectin-depolymerization capacity and suitability for d-galacturonic acid production. *Bioprocess Biosyst. Eng.* **2020**, *43*, 1549–1560. [CrossRef]
4. Rerop, Z.S.; Stellner, N.I.; Graban, P.; Haack, M.; Mehlmer, N.; Masri, M.; Brück, T.B. Bioconversion of a lignocellulosic hydrolysate to single cell oil for biofuel production in a cost-efficient fermentation process. *Fermentation* **2023**, *9*, 189. [CrossRef]
5. Koruyucu, A.; Blums, K.; Peest, T.; Schmack-Rauscher, L.; Brück, T.; Weuster-Botz, D. High-cell-density yeast oil production with diluted substrates imitating microalgae hydrolysate using a membrane bioreactor. *Energies* **2023**, *16*, 1757. [CrossRef]
6. Hernández, D.; Riaño, B.; Coca, M.; García-González, M.C. Saccharification of carbohydrates in microalgal biomass by physical, chemical and enzymatic pre-treatments as a previous step for bioethanol production. *Chem. Eng. J.* **2015**, *262*, 939–945. [CrossRef]
7. Koruyucu, A.; Schädler, T.; Gniffke, A.; Mundt, K.; Krippendorf, S.; Urban, P.; Blums, K.; Halim, B.; Brück, T.; Weuster-Botz, D. Energy-efficient production of *Microchloropsis salina* biomass with high CO_2 fixation yield in open thin-layer cascade photobioreactors. *Processes* **2024**, *12*, 1303. [CrossRef]
8. Brenner, A.; Abeliovich, A. Water purification: Algae in wastewater oxidation ponds. In *Handbook of Microalgal Culture*; John Wiley & Sons, Ltd.: Hoboken, NJ, USA, 2013; pp. 595–601.
9. Kaplan, D. Absorption and adsorption of heavy metals by microalgae. In *Handbook of Microalgal Culture*; John Wiley & Sons: Hoboken, NJ, USA, 2013; pp. 602–611.
10. Meo, A.; Priebe, X.L.; Weuster-Botz, D. Lipid production with *Trichosporon oleaginosus* in a membrane bioreactor using microalgae hydrolysate. *J. Biotechnol.* **2017**, *241*, 1–10. [CrossRef]
11. Younes, S.; Bracharz, F.; Awad, D.; Qoura, F.; Mehlmer, N.; Brueck, T. Microbial lipid production by oleaginous yeasts grown on *Scenedesmus obtusiusculus* microalgae biomass hydrolysate. *Bioprocess Biosyst. Eng.* **2020**, *43*, 1629–1638. [CrossRef]

12. Schädler, T.; Caballero Cerbon, D.; de Oliveira, L.; Garbe, D.; Brück, T.; Weuster-Botz, D. Production of lipids with *Microchloropsis salina* in open thin-layer cascade photobioreactors. *Bioresour. Technol.* **2019**, *289*, 121682. [CrossRef]

13. Boussiba, S.; Vonshak, A.; Cohen, Z.; Avissar, Y.; Richmond, A. Lipid and biomass production by the halotolerant microalga *Nannochloropsis salina*. *Biomass* **1987**, *12*, 37–47. [CrossRef]

14. Zittelli, G.C.; Rodolfi, L.; Bassi, N.; Biondi, N.; Tredici, M.R. Photobioreactors for microalgal biofuel production. In *Algae for Biofuels and Energy*; Borowitzka, M.A., Moheimani, N.R., Eds.; Springer: Dordrecht, The Netherlands, 2013; pp. 115–131.

15. Andersen, R.A. The microalgal cell. In *Handbook of Microalgal Culture*; John Wiley & Sons: Hoboken, NJ, USA, 2013; pp. 1–20.

16. Spiden, E.M.; Yap, B.H.J.; Hill, D.R.A.; Kentish, S.E.; Scales, P.J.; Martin, G.J.O. Quantitative evaluation of the ease of rupture of industrially promising microalgae by high pressure homogenization. *Bioresour. Technol.* **2013**, *140*, 165–171. [CrossRef]

17. Scholz, M.J.; Weiss, T.L.; Jinkerson, R.E.; Jing, J.; Roth, R.; Goodenough, U.; Posewitz, M.C.; Gerken, H.G. Ultrastructure and composition of the *Nannochloropsis gaditana* cell wall. *Eukaryot. Cell* **2014**, *13*, 1450–1464. [CrossRef] [PubMed]

18. Günerken, E.; D'Hondt, E.; Eppink, M.H.M.; Garcia-Gonzalez, L.; Elst, K.; Wijffels, R.H. Cell disruption for microalgae biorefineries. *Biotechnol. Adv.* **2015**, *33*, 243–260. [CrossRef] [PubMed]

19. Chmiel, H. Aufarbeitung (Downstream Processing). In *Bioprozesstechnik*; Chmiel, H., Takors, R., Weuster-Botz, D., Eds.; Springer: Berlin/Heidelberg, Germany, 2018; pp. 299–402.

20. Moon, N.J.; Hammond, E.G.; Glatz, B.A. Conversion of cheese whey and whey permeate to oil and single-cell protein. *J. Dairy. Sci.* **1978**, *61*, 1537–1547. [CrossRef]

21. Masri, M.A.; Younes, S.; Haack, M.; Qoura, F.; Mehlmer, N.; Brück, T. A seagrass-based biorefinery for generation of single-cell oils for biofuel and oleochemical production. *Energy Technol.* **2018**, *6*, 1026–1038. [CrossRef]

22. Yousuf, A.; Sannino, F.; Addorisio, V.; Pirozzi, D. Microbial conversion of olive oil mill wastewaters into lipids suitable for biodiesel production. *J. Agric. Food Chem.* **2010**, *58*, 8630–8635. [CrossRef]

23. Yu, X.; Zheng, Y.; Dorgan, K.M.; Chen, S. Oil production by oleaginous yeasts using the hydrolysate from pretreatment of wheat straw with dilute sulfuric acid. *Bioresour. Technol.* **2011**, *102*, 6134–6140. [CrossRef]

24. Takács, I.; Murthy, S.; Smith, S.; McGrath, M. Chemical phosphorus removal to extremely low levels: Experience of two plants in the Washington, DC area. *Water Sci. Technol.* **2006**, *53*, 21–28. [CrossRef]

25. Yeh, S.W.; Ong, L.J.; Glazer, A.N.; Clark, J.H. Fluorescence properties of allophycocyanin and a crosslinked allophycocyanin trimer. *Cytometry* **1987**, *8*, 91–95. [CrossRef]

26. González López, C.V.; García, M.d.C.C.; Fernández, F.G.A.; Bustos, C.S.; Chisti, Y.; Sevilla, J.M.F. Protein measurements of microalgal and cyanobacterial biomass. *Bioresour. Technol.* **2010**, *101*, 7587–7591. [CrossRef] [PubMed]

27. Mishra, S.K.; Suh, W.I.; Farooq, W.; Moon, M.; Shrivastav, A.; Park, M.S.; Yang, J.-W. Rapid quantification of microalgal lipids in aqueous medium by a simple colorimetric method. *Bioresour. Technol.* **2014**, *155*, 330–333. [CrossRef]

28. Schlagermann, P.; Göttlicher, G.; Dillschneider, R.; Rosello-Sastre, R.; Posten, C. Composition of algal oil and its potential as biofuel. *J. Combust.* **2012**, *2012*, 285185. [CrossRef]

29. Toor, S.S.; Reddy, H.; Deng, S.; Hoffmann, J.; Spangsmark, D.; Madsen, L.B.; Holm-Nielsen, J.B.; Rosendahl, L.A. Hydrothermal liquefaction of *Spirulina* and *Nannochloropsis salina* under subcritical and supercritical water conditions. *Bioresour. Technol.* **2013**, *131*, 413–419. [CrossRef]

30. Duboc, P.; Marison, I.; von Stockar, U. Quantitative calorimetry and biochemical engineering. In *Handbook of Thermal Analysis and Calorimetry*; Kemp, R.B., Ed.; Elsevier Science B.V.: Amsterdam, The Netherlands, 1999; Volume 4, pp. 267–365.

31. Yao, S.; Mettu, S.; Law, S.Q.K.; Ashokkumar, M.; Martin, G.J.O. The effect of high-intensity ultrasound on cell disruption and lipid extraction from high-solids viscous slurries of *Nannochloropsis* sp. biomass. *Algal Res.* **2018**, *35*, 341–348. [CrossRef]

32. Kurokawa, M.; King, P.M.; Wu, X.; Joyce, E.M.; Mason, T.J.; Yamamoto, K. Effect of sonication frequency on the disruption of algae. *Ultrason. Sonochem.* **2016**, *31*, 157–162. [CrossRef]

33. McMillan, J.R.; Watson, I.A.; Ali, M.; Jaafar, W. Evaluation and comparison of algal cell disruption methods: Microwave, waterbath, blender, ultrasonic and laser treatment. *Appl. Energy* **2013**, *103*, 128–134. [CrossRef]

34. Wang, M.; Yuan, W.; Jiang, X.; Jing, Y.; Wang, Z. Disruption of microalgal cells using high-frequency focused ultrasound. *Bioresource Technology* **2014**, *153*, 315–321. [CrossRef]

35. D'Hondt, E.; Martín-Juárez, J.; Bolado, S.; Kasperoviciene, J.; Koreiviene, J.; Sulcius, S.; Elst, K.; Bastiaens, L. Cell disruption technologies. In *Microalgae-Based Biofuels and Bioproducts*; Gonzalez-Fernandez, C., Muñoz, R., Eds.; Woodhead Publishing: Sawston, UK, 2017; pp. 133–154.

36. Grima, E.M.; Acién Fernández, F.G.; Robles Medina, A. Downstream processing of cell mass and products. In *Handbook of Microalgal Culture*; John Wiley & Sons: Hoboken, NJ, USA, 2013; pp. 267–309.

37. Quesada-Salas, M.C.; Delfau-Bonnet, G.; Willig, G.; Préat, N.; Allais, F.; Ioannou, I. Optimization and comparison of three cell disruption processes on lipid extraction from microalgae. *Processes* **2021**, *9*, 369. [CrossRef]

38. Montalescot, V.; Rinaldi, T.; Touchard, R.; Jubeau, S.; Frappart, M.; Jaouen, P.; Bourseau, P.; Marchal, L. Optimization of bead milling parameters for the cell disruption of microalgae: Process modeling and application to *Porphyridium cruentum* and *Nannochloropsis oculata*. *Bioresour. Technol.* **2015**, *196*, 339–346. [CrossRef]

39. Pan, Z.; Huang, Y.; Wang, Y.; Wu, Z. Disintegration of *Nannochloropsis* sp. cells in an improved turbine bead mill. *Bioresour. Technol.* **2017**, *245*, 641–648. [CrossRef] [PubMed]

40. Kröger, M.; Klemm, M.; Nelles, M. Hydrothermal disintegration and extraction of different microalgae species. *Energies* **2018**, *11*, 450. [CrossRef]

41. Doucha, J.; Lívanský, K. Influence of processing parameters on disintegration of *Chlorella* cells in various types of homogenizers. *Appl. Microbiol. Biotechnol.* **2008**, *81*, 431–440. [CrossRef]

42. Halim, R.; Harun, R.; Danquah, M.K.; Webley, P.A. Microalgal cell disruption for biofuel development. *Appl. Energy* **2012**, *91*, 116–121. [CrossRef]

43. Lee, S.J.; Yoon, B.-D.; Oh, H.-M. Rapid method for the determination of lipid from the green alga *Botryococcus braunii*. *Biotechnol. Tech.* **1998**, *12*, 553–556. [CrossRef]

44. Grimi, N.; Dubois, A.; Marchal, L.; Jubeau, S.; Lebovka, N.I.; Vorobiev, E. Selective extraction from microalgae *Nannochloropsis* sp. using different methods of cell disruption. *Bioresour. Technol.* **2014**, *153*, 254–259. [CrossRef]

45. Yap, B.H.J.; Dumsday, G.J.; Scales, P.J.; Martin, G.J.O. Energy evaluation of algal cell disruption by high pressure homogenisation. *Bioresour. Technol.* **2015**, *184*, 280–285. [CrossRef]

46. Olmstead, I.L.D.; Kentish, S.E.; Scales, P.J.; Martin, G.J.O. Low solvent, low temperature method for extracting biodiesel lipids from concentrated microalgal biomass. *Bioresour. Technol.* **2013**, *148*, 615–619. [CrossRef]

47. Zhang, R.; Parniakov, O.; Grimi, N.; Lebovka, N.; Marchal, L.; Vorobiev, E. Emerging techniques for cell disruption and extraction of valuable bio-molecules of microalgae *Nannochloropsis* sp. *Bioprocess Biosyst. Eng.* **2019**, *42*, 173–186. [CrossRef]

48. Zuorro, A.; Miglietta, S.; Familiari, G.; Lavecchia, R. Enhanced lipid recovery from *Nannochloropsis* microalgae by treatment with optimized cell wall degrading enzyme mixtures. *Bioresour. Technol.* **2016**, *212*, 35–41. [CrossRef]

49. Ho, S.-H.; Huang, S.-W.; Chen, C.-Y.; Hasunuma, T.; Kondo, A.; Chang, J.-S. Bioethanol production using carbohydrate-rich microalgae biomass as feedstock. *Bioresour. Technol.* **2013**, *135*, 191–198. [CrossRef] [PubMed]

50. Demuez, M.; Mahdy, A.; Tomás-Pejó, E.; González-Fernández, C.; Ballesteros, M. Enzymatic cell disruption of microalgae biomass in biorefinery processes. *Biotechnol. Bioeng.* **2015**, *112*, 1955–1966. [CrossRef]

51. Gelin, F.; Boogers, I.; Noordeloos, A.A.M.; Damsté, J.S.S.; Hatcher, P.G.; Leeuw, J.W.d. Novel, resistant microalgal polyethers: An important sink of organic carbon in the marine environment? *Geochim. Cosmochim. Acta* **1996**, *60*, 1275–1280. [CrossRef]

52. Mirsiaghi, M.; Reardon, K.F. Conversion of lipid-extracted *Nannochloropsis salina* biomass into fermentable sugars. *Algal Res.* **2015**, *8*, 145–152. [CrossRef]

53. Gerken, H.G.; Donohoe, B.; Knoshaug, E.P. Enzymatic cell wall degradation of *Chlorella vulgaris* and other microalgae for biofuels production. *Planta* **2013**, *237*, 239–253. [CrossRef] [PubMed]

54. Horst, I.; Parker, B.M.; Dennis, J.S.; Howe, C.J.; Scott, S.A.; Smith, A.G. Treatment of *Phaeodactylum tricornutum* cells with papain facilitates lipid extraction. *J. Biotechnol.* **2012**, *162*, 40–49. [CrossRef] [PubMed]

55. Jeong, S.W.; Nam, S.W.; HwangBo, K.; Jeong, W.J.; Jeong, B.-r.; Chang, Y.K.; Park, Y.-I. Transcriptional regulation of cellulose biosynthesis during the early phase of nitrogen deprivation in *Nannochloropsis salina*. *Sci. Rep.* **2017**, *7*, 5264. [CrossRef]

56. Klassen, V.; Blifernez-Klassen, O.; Hoekzema, Y.; Mussgnug, J.H.; Kruse, O. A novel one-stage cultivation/fermentation strategy for improved biogas production with microalgal biomass. *J. Biotechnol.* **2015**, *215*, 44–51. [CrossRef] [PubMed]

57. Zhang, X.; Zhang, L.; Liu, H.; Cao, B.; Liu, L.; Gong, W. Structure, morphology, size and application of iron phosphate. *Rev. Adv. Mater. Sci.* **2020**, *59*, 538–552. [CrossRef]

58. Hassan, M.; Blanc, P.J.; Granger, L.-M.; Pareilleux, A.; Goma, G. Influence of nitrogen and iron limitations on lipid production by *Cryptococcus curvatus* grown in batch and fed-batch culture. *Process Biochem.* **1996**, *31*, 355–361. [CrossRef]

59. Riesenberg, D.; Schulz, V.; Knorre, W.A.; Pohl, H.D.; Korz, D.; Sanders, E.A.; Roß, A.; Deckwer, W.D. High cell density cultivation of *Escherichia coli* at controlled specific growth rate. *J. Biotechnol.* **1991**, *20*, 17–27. [CrossRef] [PubMed]

60. González-Fernández, C.; Ballesteros, M. Linking microalgae and cyanobacteria culture conditions and key-enzymes for carbohydrate accumulation. *Biotechnol. Adv.* **2012**, *30*, 1655–1661. [CrossRef] [PubMed]